Supporting Information for:

Remote-controlled regio- and diastereodifferentiating photodimerization of a dynamic helical peptide-bound 2-substituted anthracene

Daisuke Taura, Akio Urushima, Yusuke Sugioka, Naoki Ousaka† and Eiji Yashima*

Department of Molecular and Macromolecular Chemistry, Graduate School of Engineering, Nagoya University, Chikusa-ku, Nagoya 464-8603, Japan.

†Present Address: Molecular Engineering Institute, Kyushu Institute of Technology, Tobata-ku, Kitakyushu, 804-8550, Japan.

E-mail: yashima@chembio.nagoya-u.ac.jp

Table of Contents

1. Instruments and Materials.

Instruments

The melting points were measured on a Yanaco MP-500D micromelting point apparatus (Yanaco, Kyoto, Japan) and were uncorrected. The IR spectra were recorded on a JASCO FT/IR-680 spectrophotometer (JASCO, Tokyo, Japan). The NMR spectra were measured on a Bruker Ascend 500 (Bruker Biospin, Billerica, MA, USA) or a Varian 500AS (Agilent Technologies, Santa Clara, CA, USA) spectrometer operating at 500 MHz for ^{1}H and 126 MHz for ^{13}C using a Teflon-valved NMR tube (5-mm (i.d.)) (Norell Inc.). Chemical shifts are reported in parts per million (δ) downfield from tetramethylsilane (TMS) in $CDCl_3$ using a solvent residual peak as the internal standard. The absorption and CD spectra were measured in a 0.05-cm quartz cell using a JASCO V-750 spectrophotometer and a JASCO J-1500 spectropolarimeter, respectively. The temperature was controlled with a JASCO PTC-510 apparatus (+50 to –20 °C) or a liquid nitrogen-controlled quartz cell (0.1-cm) in a cryostat (+25 to –40 °C). The photoirradiation (λ > 400 nm) was performed using a 500 W xenon lamp (Ushio Optical Modulex SX-UI500XQ) through a cut-off filter (SIGMAKOKI Co., Ltd.). The temperature during the photoirradiation was controlled using an ultra-cooling reactor (UCR-150N) (Techno Sigma Co., Ltd., Okayama, Japan). The electrospray ionization (ESI) mass spectra were recorded using a JEOL JMS-T100CS mass spectrometer (JEOL, Akishima, Japan). The matrix-assisted laser desorption-ionization time-of-flight mass (MALDI-TOF-MS) spectra were measured using a Bruker autoflex maX (Bruker Daltonik, Bremen, Germany) with a positive mode using 1,8,9-anthracene triol (dithranol) as the matrix. The HPLC separation of stereoisomeric and diastereomeric photodimers was performed on a JASCO PU-2080 liquid chromatograph equipped with UV-visible (JASCO UV-2070) and CD (JASCO CD-2095) dual detectors using a COSMOSIL 5C_{18}-MS-II column (0.46 (i.d.) × 25 cm, Nacalai Tesque, Kyoto, Japan).

Materials

All starting materials and dehydrated solvents were purchased from Aldrich (Milwaukee, WI), Wako Pure Chemical Industries (Osaka, Japan) and Tokyo Chemical Industry (Tokyo, Japan) unless otherwise noted. Silica gel (SiO_2) was purchased from Kanto Chemical (Tokyo, Japan). Fmoc-Api(Boc)-OH,[S1] Boc-(Ac_6c)$_2$-OBzl,[S2] Boc-L-Val-Aib-OTg[S2] and Z-Ac_6c-OH[S3] were synthesized according to the reported methods.

2. Synthetic Procedures.

Abbreviations of chemicals:

Boc: *tert*-butoxycarbonyl,

Bzl: benzyl,

Fmoc: fluorenyl-9-methoxycarbonyl,

Aib: α-aminoisobutyric acid,

Ac_6c: 1-aminocyclohexanecarboxylic acid,

Api: 4-aminopiperidine-4-carboxylic acid,

HATU: *O*-(7-azabenzotrizol-1-yl)-1,1,3,3-tetramethyluronium hexafluorophosphate,

EDC·HCl: 1-ethyl-3-(3-dimethylaminopropyl)-carbodiimide hydrochloride,

HOAt: 7-aza-1-hydroxy-1,2,3-benzotriazole,

DIEA: *N*,*N*-diisopropylethylamine,

DMAP: 4-dimethylaminopyridine,

NMM: *N*-methylmorpholine,

Tg: 2-(2-(2-methoxyethoxy)ethoxy)ethyl,

Tfa: trifluoroacetyl,

Z: benzyloxycarbonyl.

General Procedures for the Peptide Syntheses.

Boc-, Fmoc-, Z- and Tfa-protecting groups were removed by treatment with HCO_2H or 4N HCl in 1,4-dioxane, 20% piperidine in DMF, 10% Pd-C/H_2 in MeOH and $NaBH_4$ in EtOH, respectively. The N-deprotected peptide formic acid salt was neutralized with aqueous 5% $NaHCO_3$. The resulting N-deprotected peptide and N-deprotected peptide hydrochloride salts were used without further purification unless otherwise noted. Peptide coupling reactions were carried out by HOAt/HATU, HOAt/EDC·HCl or HOBt·H_2O/EDC·HCl methods.

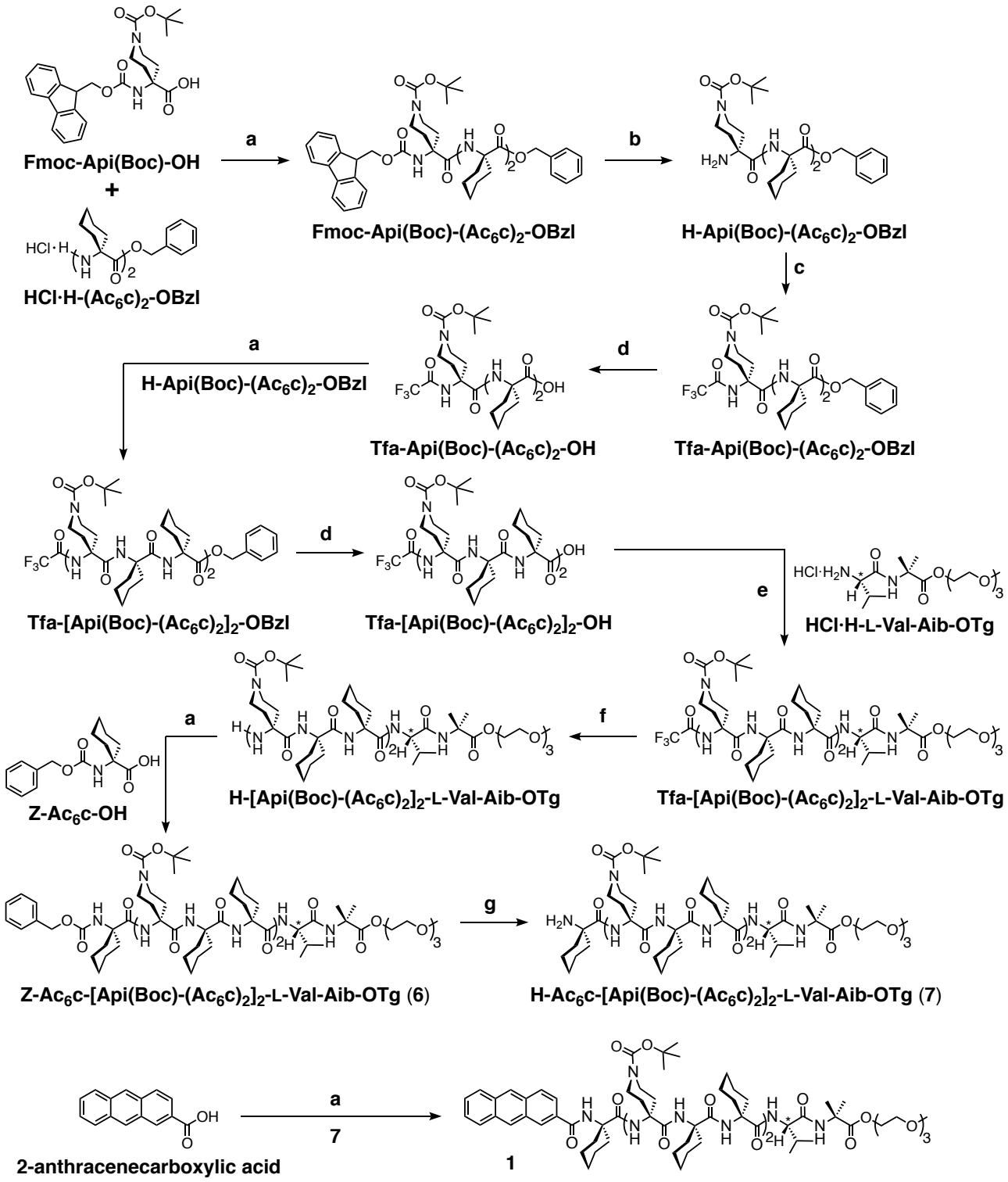

Scheme S1. Synthesis of the peptide-bound 2-substituted anthracene derivative **1**. Reagents and conditions: (a) HOAt, HATU, CH_2Cl_2, 0 °C to rt. (b) 20% piperidine in DMF, rt. (c) Trifluoroacetic anhydride, Et_3N, DMAP, CH_2Cl_2, rt. (d) 10% Pd-C/H_2, THF/H_2O, rt. (e) HOAt, EDC·HCl, DMF, 0 °C to rt. (f) $NaBH_4$, EtOH, 0 °C. (g) 10% Pd-C/H_2, MeOH, rt.

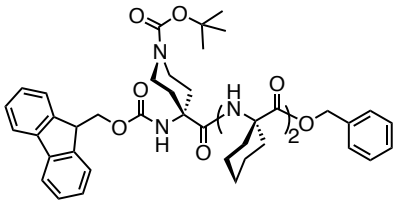

Fmoc-Api(Boc)-(Ac$_6$c)$_2$-OBzl

Fmoc-Api(Boc)-(Ac$_6$c)$_2$-OBzl. To a suspension of Fmoc-Api(Boc)-OH[S1] (1.70 g, 3.64 mmol) and HOAt (250 mg, 1.82 mmol) in dry CH_2Cl_2 (12 mL) were added HATU (1.38 g, 3.64 mmol) and DIEA (635 μL, 3.64 mmol) at 0 ºC under Ar with stirring. After 1 h, to this was added HCl·H-(Ac$_6$c)$_2$-OBzl (2.13 g, 5.47 mmol), which had been obtained by treatment of Boc-(Ac$_6$c)$_2$-OBzl[S2] with 4N HCl in 1,4-dioxane, and DIEA (950 μL, 5.47 mmol). The reaction mixture was stirred at 0 ºC for 2 h and further at room temperature for 65 h under Ar. The solution was then diluted with $CHCl_3$, and the mixture was washed with 1N aqueous HCl, 5% aqueous $NaHCO_3$ and brine, dried over $MgSO_4$, filtered and concentrated under reduced pressure. The residue was purified by column chromatography (SiO_2, $CHCl_3$/EtOAc (2/1, v/v)) and further by reprecipitation from Et_2O/*n*-hexane (1/3, v/v), affording Fmoc-Api(Boc)-(Ac$_6$c)$_2$-OBzl (2.22 g, 75.3%) as a white solid. Mp: 174–177 ºC. IR (KBr, cm^{-1}): 1734 ($\nu_{C=O}$), 1698 ($\nu_{C=O}$), 1689 ($\nu_{C=O}$), 1519 (ν_{N-H}). ^{1}H NMR (500 MHz, $CDCl_3$, 25 ºC): δ 7.79 (d, J = 7.6 Hz, 2H, ArH), 7.55–7.54 (m, 3H, ArH, NH), 7.42 (t, J = 7.5 Hz, 2H, ArH), 7.35–7.32 (m, 2H, ArH), 7.26–7.15 (m, partially overlapping with $CHCl_3$ signal), 6.19 (s, 1H, NH), 5.03 (s, 2H, CH_2), 4.70 (s, 1H, NH), 4.57 (d, J = 5.1 Hz, 2H, CH_2), 4.19 (t, J = 5.6 Hz, 1H, CH_2), 3.79 (br, 2H, CH_2), 2.75 (br, 2H, CH_2), 2.08–1.22 (m, partially overlapping with H_2O signal). ^{13}C NMR (126 MHz, $CDCl_3$, 25 ºC): δ 174.20, 173.14, 172.86, 155.06, 154.51, 143.38, 141.48, 136.41, 128.56, 128.35, 127.98, 127.96, 127.23, 124.54, 120.18, 79.99, 66.64, 66.44, 60.19, 58.73, 58.43, 47.26, 32.26, 31.88, 28.40, 25.29, 25.11, 21.37, 21.32. HRMS (ESI+): m/z calcd for (M+Na$^+$), 829.4152; found, 829.4125.

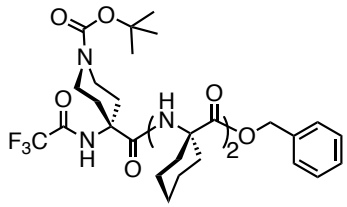

Tfa-Api(Boc)-(Ac$_6$c)$_2$-OBzl

Tfa-Api(Boc)-(Ac$_6$c)$_2$-OBzl. To a solution of H-Api(Boc)-(Ac$_6$c)$_2$-OBzl (381 mg, 0.650 mmol), which had been obtained by treatment of Fmoc-Api(Boc)-(Ac$_6$c)$_2$-OBzl with 20% piperidine in DMF, in dry CH_2Cl_2 (11 mL) were added trifluoroacetic anhydride (0.150 mL, 1.06 mmol), Et_3N (0.150 mL, 1.08 mmol) and DMAP (16.6 mg, 0.136 mmol) at room temperature under Ar with

stirring. The reaction mixture was stirred at room temperature for 2 h. The solution was then diluted with $CHCl_3$, and the mixture was washed with 5% aqueous $NaHCO_3$ and brine, dried over $MgSO_4$, filtered and concentrated under reduced pressure. The residue was purified by column chromatography (SiO_2, $CHCl_3$/EtOAc (3/1, v/v)) and further by reprecipitation from Et_2O/*n*-hexane (1/5, v/v), affording Tfa-Api(Boc)-$(Ac_6c)_2$-OBzl (298 mg, 67.2%) as a white solid. Mp: 172–174 ºC. IR (KBr, cm^{-1}): 1734 ($\nu_{C=O}$), 1698 ($\nu_{C=O}$), 1671 ($\nu_{C=O}$), 1508 (ν_{N-H}). ^1H NMR (500 MHz, $CDCl_3$, 50 ºC): δ 7.33–7.29 (m, 5H, ArH, NH), 6.43 (s, 1H, NH), 6.13 (s, 1H, NH), 5.08 (s, 2H, CH_2), 3.83–3.80 (m, 2H, CH_2), 3.08–3.03 (m, 2H, CH_2), 2.09–1.97 (m, 8H, CH_2), 1.84–1.79 (m, 4H, CH_2), 1.64–1.56 (m, partially overlapping with H_2O signal), 1,46 (s, 9H, CH_3), 1.43–1.40 (m, 11H, CH_2), 1.33–1.23 (m, 4H, CH_2). ^{13}C NMR (126 MHz, $CDCl_3$, 50 ºC): δ 173.98, 172.68, 170.98, 157.95, 157.65, 157.35, 157.05, 154.50, 136.50, 128.51, 128.43, 128.05, 118.91, 116.62, 114.32, 112.02, 80.40, 66.76, 60.83, 59.95, 58.95, 39.35, 32.45, 32.21, 31.69, 20.45, 25.28, 25.13, 21.52, 21.46. HRMS (ESI+): *m*/*z* calcd for ($M+Na^+$), 703.3295; found, 703.3300.

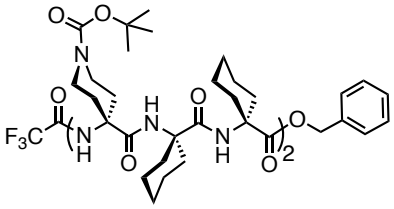

Tfa-[Api(Boc)-$(Ac_6c)_2$]$_2$-OBzl

Tfa-[Api(Boc)-$(Ac_6c)_2$]$_2$-OBzl. To a suspension of Tfa-Api(Boc)-$(Ac_6c)_2$-OH (296 mg, 0.507 mmol), which had been obtained by treatment of Tfa-Api(Boc)-$(Ac_6c)_2$-OBzl with 10% Pd-C/H_2 in THF/H_2O (10/1, v/v), and HOAt (35.2 mg, 0.254 mmol) in dry CH_2Cl_2 (2 mL) were added HATU (214 mg, 0.559 mmol) and DIEA (110 µL, 0.615 mmol) at 0 ºC under Ar with stirring. After 1 h, to this was added H-Api(Boc)-$(Ac_6c)_2$-OBzl (108 mg, 76.0 µmol). The reaction mixture was stirred at 0 ºC for 1 h and further at room temperature for 134 h under Ar. The solution was then diluted with $CHCl_3$, and the mixture was washed with 1N aqueous HCl, 5% aqueous $NaHCO_3$ and brine, dried over $MgSO_4$, filtered and concentrated under reduced pressure. The residue was washed with *n*-hexane, affording Tfa-[Api(Boc)-$(Ac_6c)_2$]$_2$-OBzl (519 mg, 89.6%) as a white solid. Mp: 222–223 ºC. IR (KBr, cm^{-1}): 1734 ($\nu_{C=O}$), 1700 ($\nu_{C=O}$), 1671 ($\nu_{C=O}$), 1523 (ν_{N-H}). ^1H NMR (500 MHz, $CDCl_3$, 50 ºC): δ 8.24 (s, 1H, NH), 7.33–7.22 (m, partially overlapping with $CHCl_3$ signal), 6.97 (s, 1H, NH), 6.66 (s, 1H, NH), 6.56 (s, 1H, NH), 5.10 (s, 2H, CH_2), 3.92–3.86 (m, 4H, CH_2), 3.22–3.18 (t, J = 11.3 Hz, 2H, CH_2), 3.01–2.77 (br, 2H, CH_2), 2.16–1.20 (m, partially overlapping with H_2O signal). ^{13}C NMR (126 MHz, $CDCl_3$, 50 ºC): δ 175.04, 174.58, 174.56, 173.19, 173.13, 171.92, 158.59, 158.29, 155.30, 154.48, 136.78, 128.26, 127.96, 127.62, 116.62, 114.33, 80.61, 79.76, 66.22, 60.78,

59.87, 59.84, 59.15, 59.09, 58.43, 39.40, 32.68, 28.50, 28.45, 25.66, 25.64, 25.22, 25.02, 21.79, 21.72, 21.65, 21.50. HRMS (ESI+): *m*/*z* calcd for ($M+Na^+$), 1179.6293; found, 1179.6269.

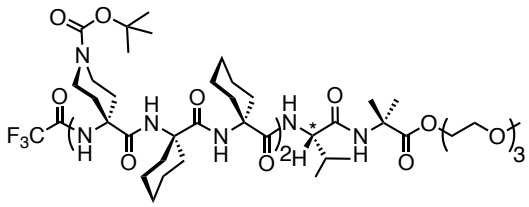

Tfa-[Api(Boc)-$(Ac_6c)_2]_2$-L-Val-Aib-OTg

Tfa-[Api(Boc)-$(Ac_6c)_2]_2$-L-Val-Aib-OTg. To a suspension of Tfa-[Api(Boc)-$(Ac_6c)_2]_2$-OH (352 mg, 0.328 mmol) and HCl·H-L-Val-Aib-OTg (158 mg, 0.394 mmol), which had been obtained by treatments of Tfa-[Api(Boc)-$(Ac_6c)_2]_2$-OBzl with 10% Pd-C/H_2 in THF/H_2O (10/1, v/v) and Boc-L-Val-Aib-OTg[S2] with 4N HCl in 1,4-dioxane, respectively, and HOAt (51.6 mg, 0.377 mmol) in dry DMF (4 mL) was added EDC·HCl (66.8 mg, 0.328 mmol) at 0 °C under Ar with stirring. After 1 h, to this was added NMM (47.0 μL, 0.410 mmol) at 0 ºC under Ar with stirring. The reaction mixture was stirred at 0 ºC for 2.5 h and further at room temperature for 20 h under Ar. The solution was then diluted with $CHCl_3$, and the mixture was washed with 1N aqueous HCl, 5% aqueous $NaHCO_3$ and brine, dried over $MgSO_4$, filtered and concentrated under reduced pressure. The residue was washed with Et_2O/*n*-hexane (1/4, v/v), affording Tfa-[Api(Boc)-$(Ac_6c)_2]_2$-L-Val-Aib-OTg (454 mg, 98.5%) as a white solid. Mp: 145–147 ºC. IR (KBr, cm^{-1}): 1735 ($\nu_{C=O}$), 1700 ($\nu_{C=O}$), 1663 ($\nu_{C=O}$), 1523 (ν_{N-H}). ^1H NMR (500 MHz, $CDCl_3$, 25 ºC): δ 7.98 (s, 1H, NH), 7.30–7.25 (m, partially overlapping with $CHCl_3$ signal), 7.02 (s, 1H, NH), 6.75 (s, 1H, NH), 6.64 (s, 1H, NH), 4.28–4.17 (m, 3H, OCH_2, CH_2), 3.86 (m, 4H, CH_2), 3.70–3.61 (m, 8H, OCH_2), 3.54–3.52 (m, 2H, OCH_2), 3.36 (s, 3H, OCH_3), 3.26–3.20 (m, 2H, CH_2), 3.12 (t, J = 11.0 Hz. 1H, CH_2), 2.78 (t, 1H, J = 12.0 Hz, CH_2), 2.51–2.49 (m, 1H, CH_2), 2.42–2.35 (m, 1H, CH_2), 2.25–1.20 (m, partially overlapping with H_2O signal), 0.98 (dd, J = 20.6, 6.8 Hz, 6H, CH_3). ^{13}C NMR (126 MHz, $CDCl_3$, 50 ºC): δ 176.19, 175.79, 175.42, 174.95, 174.41, 174.07, 172.87, 172.16, 158.76, 158.46, 155.02, 154.62, 116.72, 114.43, 80.24, 79.81, 72.10, 70.75, 70.63, 69.05, 63.90, 61.13, 60.37, 60.00, 59.81, 59.33, 59.17, 58.98, 57.65, 56.07, 39.82, 39.47, 34.60, 31.45, 29.86, 29.23, 28.54, 28.49, 25.71, 25.55, 25.26, 24.42, 22.15, 21.97, 21.81, 21.56, 21.42, 19.42, 19.35. HRMS (ESI+): *m*/*z* calcd for ($M+Na^+$), 1419.7978; found, 1419.7982.

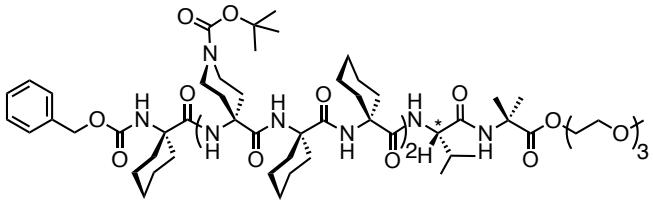

Z-Ac$_6$c-[Api(Boc)-(Ac$_6$c)$_2$]$_2$-L-Val-Aib-OTg (6)

Z-Ac$_6$c-[Api(Boc)-(Ac$_6$c)$_2$]$_2$-L-Val-Aib-OTg (6). To a suspension of Z-Ac$_6$c-OH[S3] (72.8 mg, 0.265 mmol) and HOAt (12.9 mg, 88.3 μmol) in dry CH_2Cl_2 (1 mL) were added HATU (74.1 mg, 0.194 mmol) and DIEA (37.0 μL, 0.214 mmol) at 0 °C under Ar with stirring. After 1.5 h, to this was added H-[Api(Boc)-(Ac$_6$c)$_2$]$_2$-L-Val-Aib-OTg (218 mg, 0.177 mmol), which had been obtained by treatment of Tfa-[Api(Boc)-(Ac$_6$c)$_2$]$_2$-L-Val-Aib-OTg with $NaBH_4$ in EtOH, at 0 ºC under Ar with stirring. The reaction mixture was stirred at 0 ºC for 2 h and further at room temperature for 67 h under Ar. The solution was then diluted with $CHCl_3$, and the mixture was washed with 1N aqueous HCl, 5% aqueous $NaHCO_3$ and brine, dried over $MgSO_4$, filtered and concentrated under reduced pressure. The residue was purified by column chromatography (SiO_2, $CHCl_3$/EtOAc/MeOH (5/4/1, v/v/v)) and further by recrystalization from $CHCl_3$/Et_2O (1/12, v/v), affording Z-Ac$_6$c-[Api(Boc)-(Ac$_6$c)$_2$]$_2$-L-Val-Aib-OTg (**6**) (239 mg, 91.3%) as a white solid. Mp: 137–140 ºC. IR (KBr, cm^{-1}): 1736 ($\nu_{C=O}$), 1699 ($\nu_{C=O}$), 1662 ($\nu_{C=O}$), 1523 (ν_{N-H}). ^{1}H NMR (500 MHz, $CDCl_3$, 50 ºC): δ 7.39–7.29 (m, 9H, ArH, NH), 7.14 (s, 1H, NH), 7.06 (s, 1H, NH), 7.05 (s, 1H, NH), 6.79 (s, 1H, NH), 5.90 (s, 1H, NH), 5.15 (dd, J = 36.8, 12.6 Hz, 2H, CH_2), 4.29–4.16 (m, 3H, CH_2), 3.87–3.76 (m, 4H, CH_2), 3.69–3.61 (m, 8H, CH_2), 3.54–3.52 (m, 2H, CH_2), 3.36 (s, 3H, OCH_3), 3.23 (t, J = 12.2 Hz, 1H, CH_2), 3.07 (t, J = 11.0 Hz, 1H, CH_2), 2.96 (t, J = 10.7 Hz, 1H, CH_2), 2.87 (t, J = 11.4 Hz, 1H, CH_2), 2.52–2.49 (m, 1H, CH_2), 2.41–2.35 (m, 1H, CH), 2.20–1.14 (m, partially overlapping with H_2O signal), 0.98 (dd, J = 23.9, 6.9 Hz, 6H, CH_3). ^{13}C NMR (126 MHz, $CDCl_3$, 50 ºC): δ 176.20, 175.80, 175.62, 175.37, 175.31, 174.82, 174.60, 174.01, 171.94, 156.32, 154.85, 154.64, 136.64, 128.68, 128.28, 127.26, 80.00, 79.52, 72.06, 70.71, 70.56, 69.04, 66.84, 63.88, 60.40, 60.11, 60.00, 59.80, 59.48, 59.34, 58.96, 57.73, 57.30, 55.85, 39.82, 39.16, 34.81, 29.67, 28.55, 28.47, 25.70, 25.56, 25.50, 25.34, 25.09, 24.59, 22.09, 22.02, 21.92, 21.77, 21.61, 21.56, 21.46, 19.49, 18.92. HRMS (ESI+): m/z calcd for (M+Na$^+$), 1583.9395; found, 1583.9353.

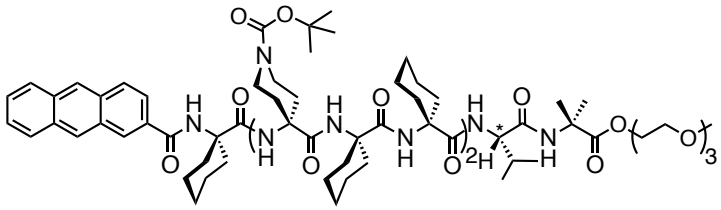

1

1. To a suspension of 2-anthracenecarboxylic acid (23.7 mg, 0.107 mmol) and HOAt (7.36 mg, 54.1 μmol) in dry CH_2Cl_2 (2 mL) were added HATU (45.1 mg, 0.119 mmol) and DIEA (22.0 μL, 0.126 mmol) at 0 ºC under Ar with stirring. After 2 h, to this was added H-Ac_6c-[Api(Boc)-(Ac_6c)$_2$]$_2$-L-Val-Aib-OTg (**7**) (108 mg, 76.0 μmol), which had been obtained by treatment of Z-Ac_6c-[Api(Boc)-(Ac_6c)$_2$]$_2$-L-Val-Aib-OTg (**6**) with 10% Pd-C/H_2 in MeOH. The reaction mixture was stirred at 0 ºC for 2 h and further at room temperature for 88 h under Ar. The solution was then diluted with $CHCl_3$, and the mixture was washed with 1N aqueous HCl, 5% aqueous $NaHCO_3$ and brine, dried over $MgSO_4$, filtered and concentrated under reduced pressure. The residue was purified by column chromatography (SiO_2, $CHCl_3$/MeOH (9/1, v/v) and EtOAc), affording **1** (98.7 mg, 79.7%) as a pale yellow solid. Mp: 157–159 ºC. IR (KBr, cm^{-1}): 1736 ($\nu_{C=O}$), 1661 ($\nu_{C=O}$), 1523 (ν_{N-H}). ^{1}H NMR (500 MHz, $CDCl_3$, 25 °C): δ 8.58 (s, 1H, ArH), 8.53 (s, 1H ArH), 8.51 (s, 1H ArH), 8.13 (d, J = 9.0 Hz, 1H, ArH), 8.08–8.06 (m, 2H, ArH), 7.75 (dd, J = 8.9, 1.7 Hz, 1H, ArH), 7.61–7.55 (m, 2H, ArH), 7.52 (s, 1H, NH), 7.39 (s, 1H, NH), 7.36 (s, 1H, NH), 7.30 (m, partially overlapping with $CHCl_3$ signal), 7.18 (s, 1H, NH), 7.06 (s, 1H, NH), 6.90 (s, 1H, NH), 6.68 (s, 1H, NH), 4.30–4.18 (m, 3H, OCH_2, CH), 3.95–3.92 (m, 4H, CH_2), 3.70–3.63 (m, 8H, OCH_2), 3.55–3.53 (m, 2H, OCH_2), 3.37 (s, 3H, OCH_3), 3.27 (br s, 1H, CH_2), 3.10 (t, J = 12 Hz, 1H, CH_2), 2.98 (m, 1H, CH_2), 2.84 (br s, 1H, CH_2), 2.52–2.49 (m, 1H, CH_2), 2.45–2.41 (m, 1H, CH_2), 2.21–1.13 (m, partially overlapping with H_2O signal), 0.98 (dd, J = 33.0, 6.9 Hz, 6H, CH_3). ^{13}C NMR (126 MHz, $CDCl_3$, 25 °C): δ 176.28, 175.90, 175.79, 175.64, 174.97, 174.77, 174.66, 174.12, 171.82, 168.00, 154.86, 154.58, 133.10, 132.28, 132.25, 130.21, 129.57, 129.44, 129.27, 128.55, 128.45, 128.23, 126.75, 126.42, 126.18, 122.50, 122.30, 79.97, 79.53, 71.89, 70.56, 70.50, 70.43, 68.82, 63.85, 60.22, 59.84, 59.40, 58.99, 57.56, 57.40, 55.70, 39.70, 35.21, 34.13, 31.59, 29.46, 28.50, 28.40, 25.57, 25.38, 25.24, 25.15, 24.41, 22.66, 22.22, 21.90, 21.66, 21.33, 19.47, 18.75, 14.12. HRMS (ESI+): m/z calcd for ($M+Na^+$), 1652.9571; found, 1652.9584.

3. General Procedures for Photodimerization of 1.

A typical experimental procedure is described below. Stock solutions of **1** (0.20 mM; solution I) and 1,1,2,2-tetrachloroethane (0.20 mM; solution II) in CD_3CN were prepared. An aliquot of solution I (0.15 μmol, 750 μL) was added into a Teflon-valved NMR tube (5-mm (i.d.)) by a syringe. After the solvent was removed under reduced pressure, to this was added an aliquot of solution II (0.15 μmol, 750 μL) by a syringe. The solution was degassed five times by means of freeze-pump out-thaw (nitrogen) cycles, and then irradiated with light (> 400 nm) at 25 °C for 120 min under nitrogen using a cut-off filter. The reaction progress was monitored by ^{1}H NMR spectroscopy (Fig. S5a). The conversion of **1** was determined by ^{1}H NMR spectroscopy (Fig. S5a,b). In the same way, the photodimerizations of **1** were performed in degassed CD_3CN (0.20 mM and 1.0 mM) at various temperatures (Figs. S4 and S6–S11). The relative yields of four stereoisomers (*anti*-HT-**2**, *syn*-HT-**3**, *anti*-HH-**4** and *syn*-HH-**5**) and the diastereoselectivity (diastereomeric excess (de)) of *syn*-HT-**3** and *anti*-HH-**4** photodimers were determined by HPLC analyses (see below).

4. Isolation of Stereoisomers and Diastereomers, and Structure Determination.

The four stereoisomers obtained after photoirradiation (> 400 nm) of **1** (0.20 mM) in degassed CD_3CN at 25 °C (Fig. S5a) were first separated into five fractions (fr.1–fr.5) by HPLC fractionation (Fig. 2a) (HPLC conditions: column, COSMOSIL 5C_{18}-MS-II (0.46 (i.d.) × 25 cm); eluent, CH_3CN/CH_3OH (75/25 (v/v)); flow rate, 1.0 mL/min; column temperature, 25 °C; detection, UV absorption at 254 nm and CD at 300 nm.). The fr.2 was a mixture of diastereomers ((*P*)-*anti*-HH-**4** and (*M*)-*anti*-HH-**4**), which were then further separated into two fractions (fr.2-1 and fr.2-2) by HPLC fractionation (Fig. 2b) (HPLC conditions: column, COSMOSIL 5C_{18}-MS-II (0.46 (i.d.) × 25 cm); eluent, CH_3OH/H_2O (95/5 (v/v)); flow rate, 1.0 mL/min; column temperature, 25 °C; detection, UV absorption at 254 nm and CD at 300 nm.). The ^{1}H NMR spectra of the isolated photodimers are shown in Fig. S1. The absolute configurations of the two chiral photodimers (*syn*-HT-**3** and *anti*-HH-**4**) were determined based on their CD spectra measured in CH_3OH by comparing the calculated ones of the corresponding chiral photodimers of 2-anthracenecarboxylic acid reported by Inoue and co-workers.[S4] The positive-mode MALDI-TOF-MS spectra of the separated fractions (fr.1, fr.2-1, fr.4 and fr.5) also showed molecular ionic peaks at m/z = 3282.82 – 3282.93 ($[C_{176}H_{262}N_{22}O_{36} + Na]^+$), indicating the formation of cyclophotodimers (Fig. S2).

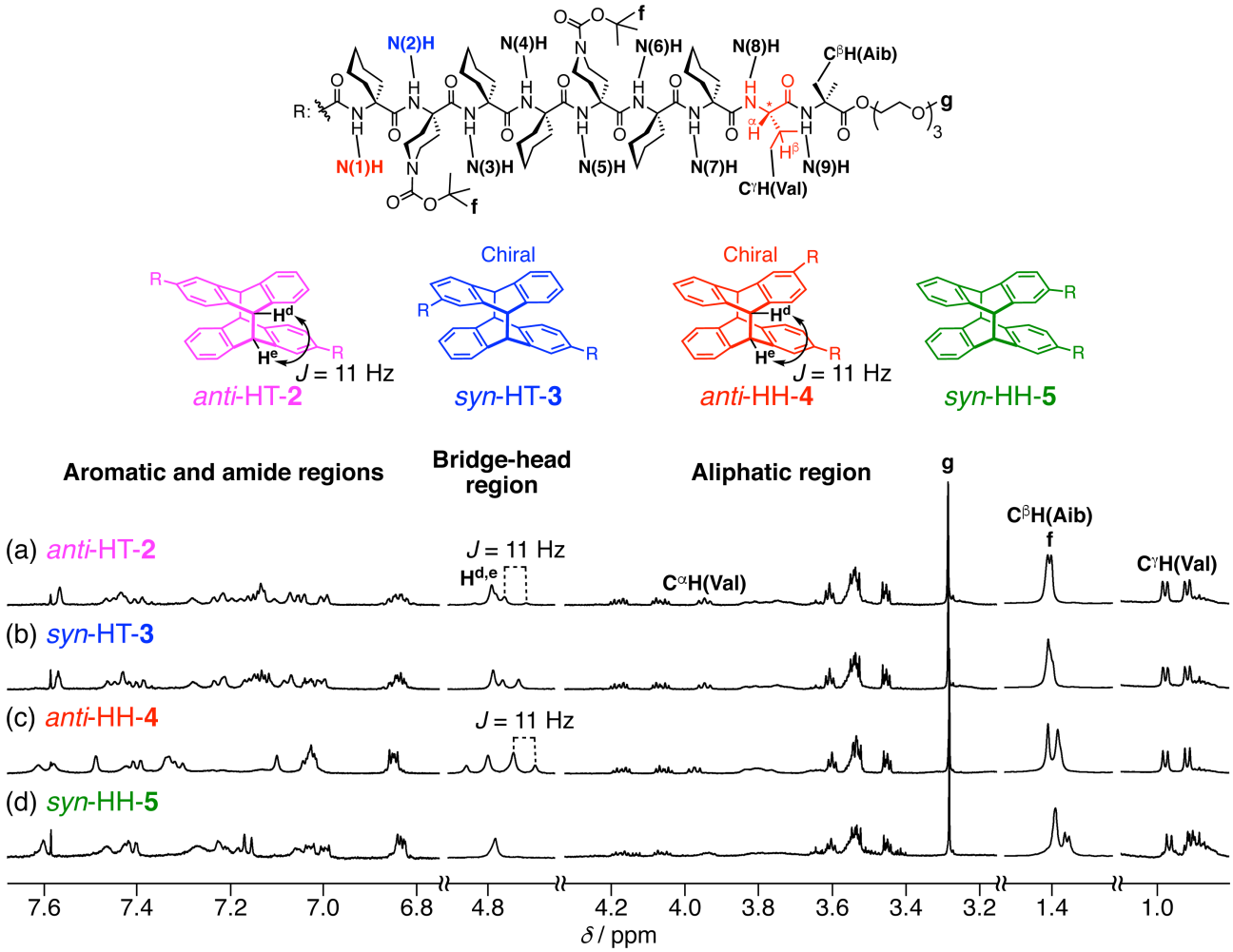

Fig. S1 Partial ^{1}H NMR spectra (500 MHz, CD_3CN, 25 °C) of isolated *anti*-HT-**2** (a), *syn*-HT-**3** (b), *anti*-HH-**4** (c) and *syn*-HH-**5** (d).

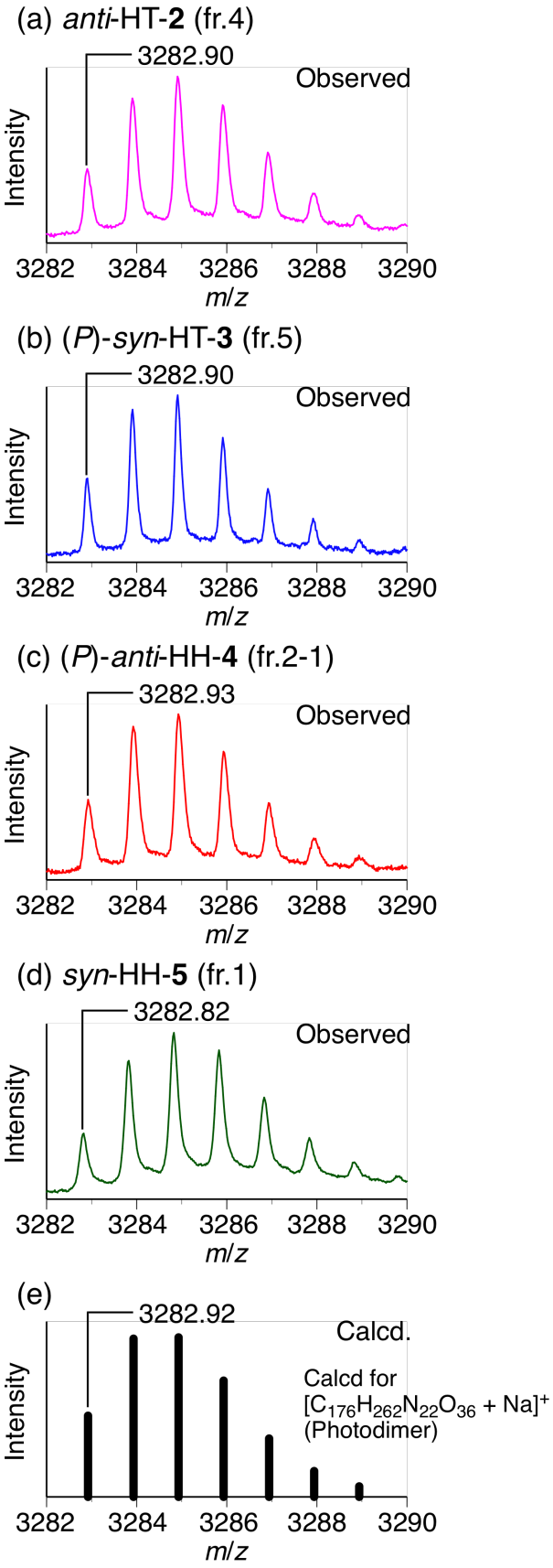

Fig. S2 Positive-mode MALDI-TOF-MS spectra of *anti*-HT-**2** (a), (*P*)-*syn*-HT-**3** (b), (*P*)-*anti*-HH-**4** (c) and *syn*-HH-**5** (d) and their calculated one (e).

5. Temperature-Dependent CD and Absorption Spectral Changes of 6 in CH_3CN.

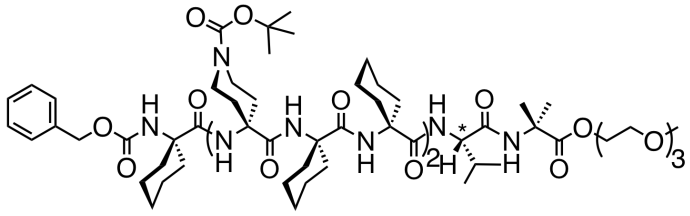

Z-Ac$_6$c-[Api(Boc)-(Ac$_6$c)$_2$]$_2$-L-Val-Aib-OTg (6)

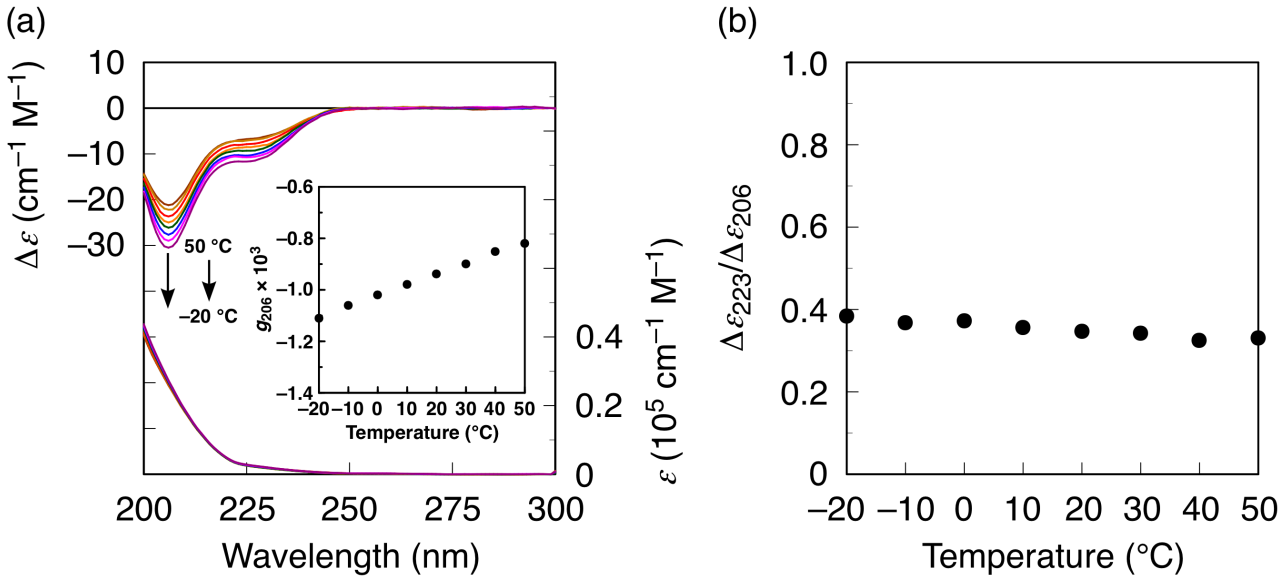

Fig. S3 (a) Temperature-dependent CD and absorption spectral changes of Z-Ac$_6$c-[Api(Boc)-(Ac$_6$c)$_2$]$_2$-L-Val-Aib-OTg (**6**) in CH_3CN (0.20 mM). Inset shows the plots of the *g*-value (g_{206} = $\Delta\varepsilon_{206}/\varepsilon_{206}$) at 206 nm. (b) Plots of the molar CD ratio at 223 and 206 nm ($\Delta\varepsilon_{223}$ and $\Delta\varepsilon_{206}$) of **6** versus temperature.

6. Photodimerization of 1 and Its Kinetic Study.

6-1. Photodimerization of 1 in Degassed CD_3CN at Various Temperatures (runs 1–8, Table 1).

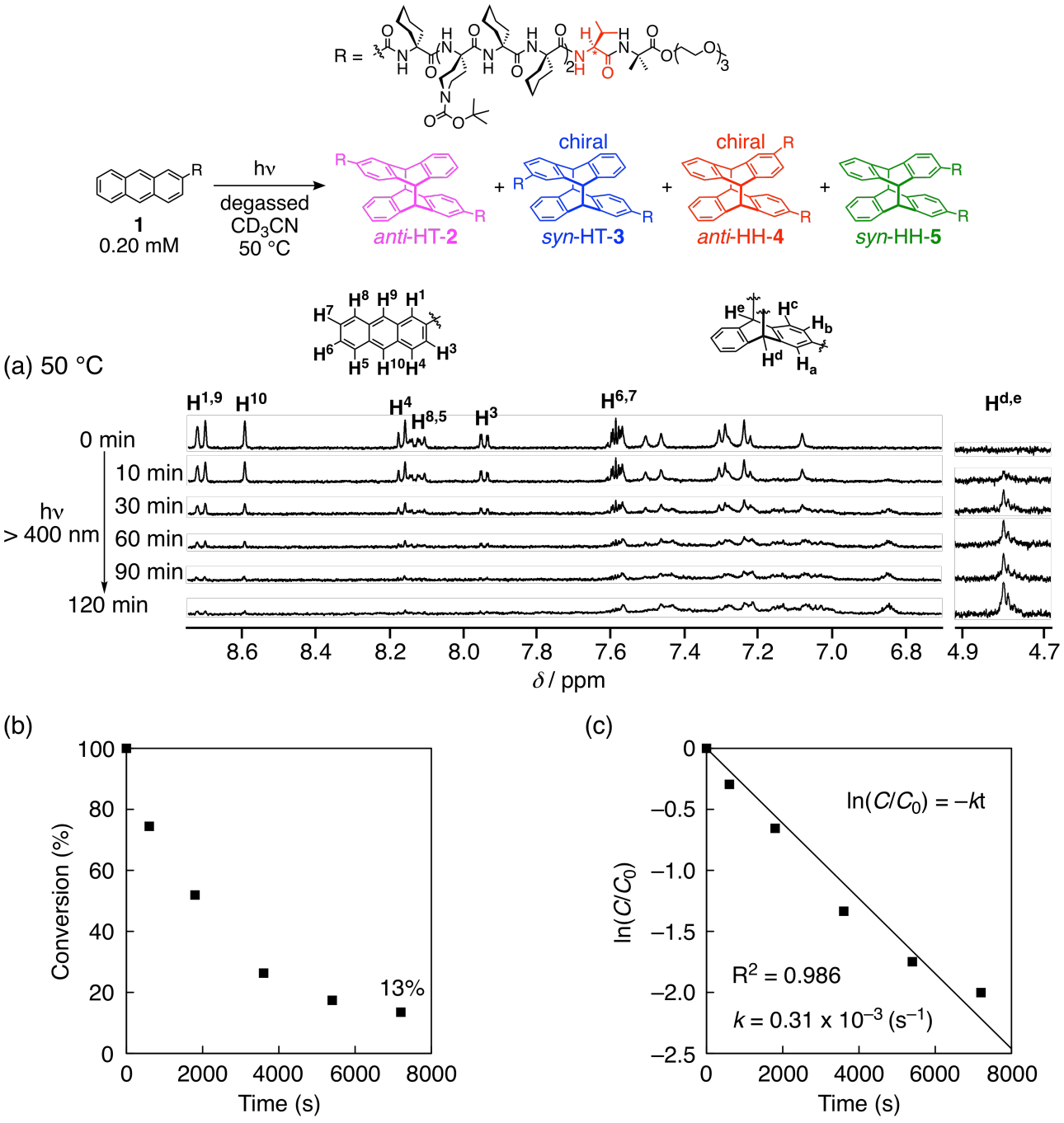

Fig. S4 (a) Time-dependent ^{1}H NMR spectral changes of **1** (500 MHz, degassed CD_3CN, 0.20 mM) upon light irradiation (> 400 nm) at 50 °C (run 1, Table 1) measured at 25 °C. The peak assignments of the anthracene unit were done on the basis of the *g*COSY and ROESY (Fig. S14) spectra measured in CD_3CN. (b,c) Time-conversion relationships (b) and kinetic plots (c) of the photodimerization of **1** (degassed CD_3CN, 50 °C, 0.20 mM) estimated from the integral ratios of the peaks for H^{10} (**1**) and 1,1,2,2-tetrachloroethane used as the internal standard on the basis of the ^{1}H NMR spectral changes shown in (a).

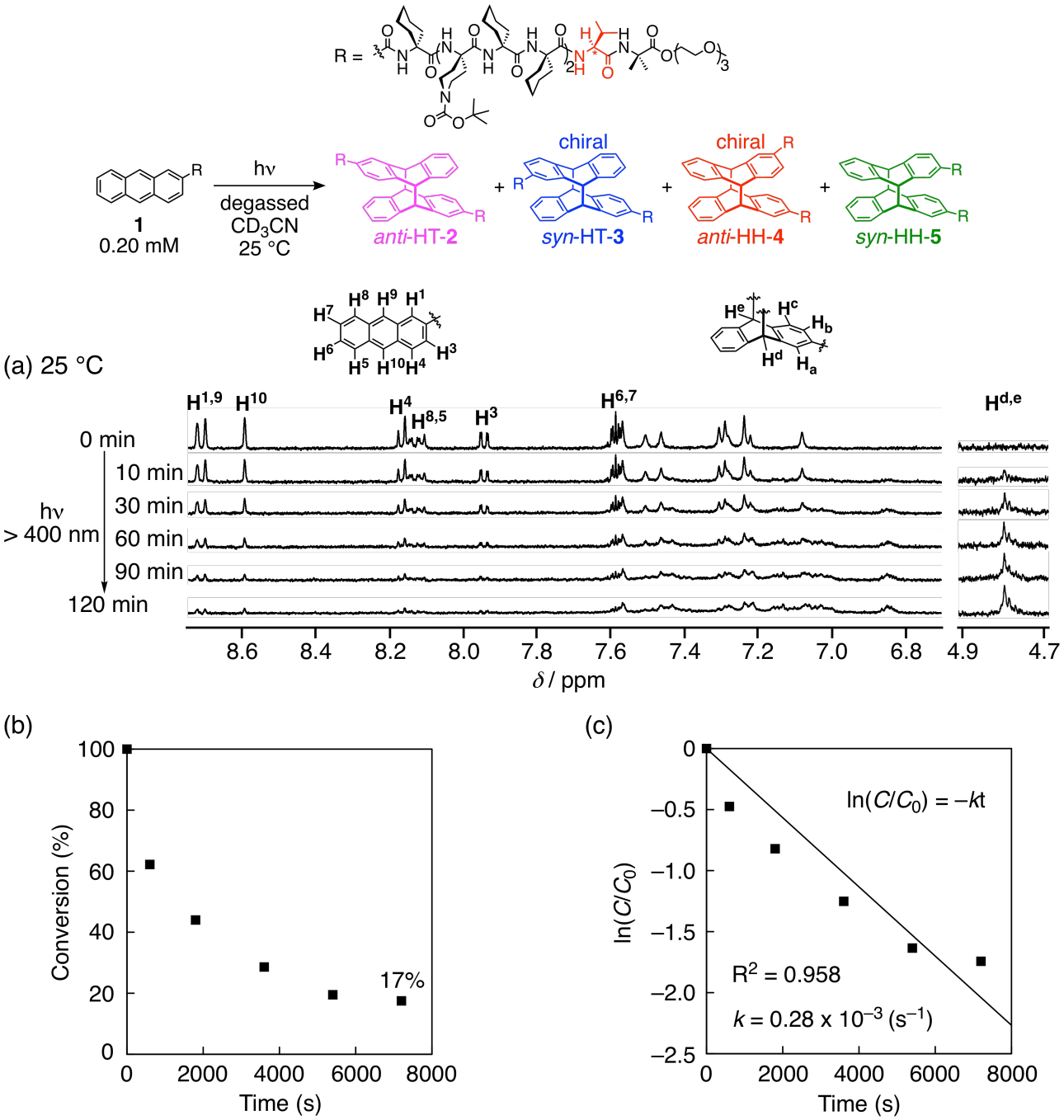

Fig. S5 (a) Time-dependent ^{1}H NMR spectral changes of **1** (500 MHz, degassed CD_3CN, 25 °C, 0.20 mM) upon light irradiation (> 400 nm) at 25 °C (run 2, Table 1). The peak assignments of the anthracene unit were done on the basis of the *g*COSY and ROESY (Fig. S14) spectra measured in CD_3CN. (b,c) Time-conversion relationships (b) and kinetic plots (c) of the photodimerization of **1** (degassed CD_3CN, 25 °C, 0.20 mM) estimated from the integral ratios of the peaks for H^{10} (**1**) and 1,1,2,2-tetrachloroethane used as the internal standard on the basis of the ^{1}H NMR spectral changes shown in (a).

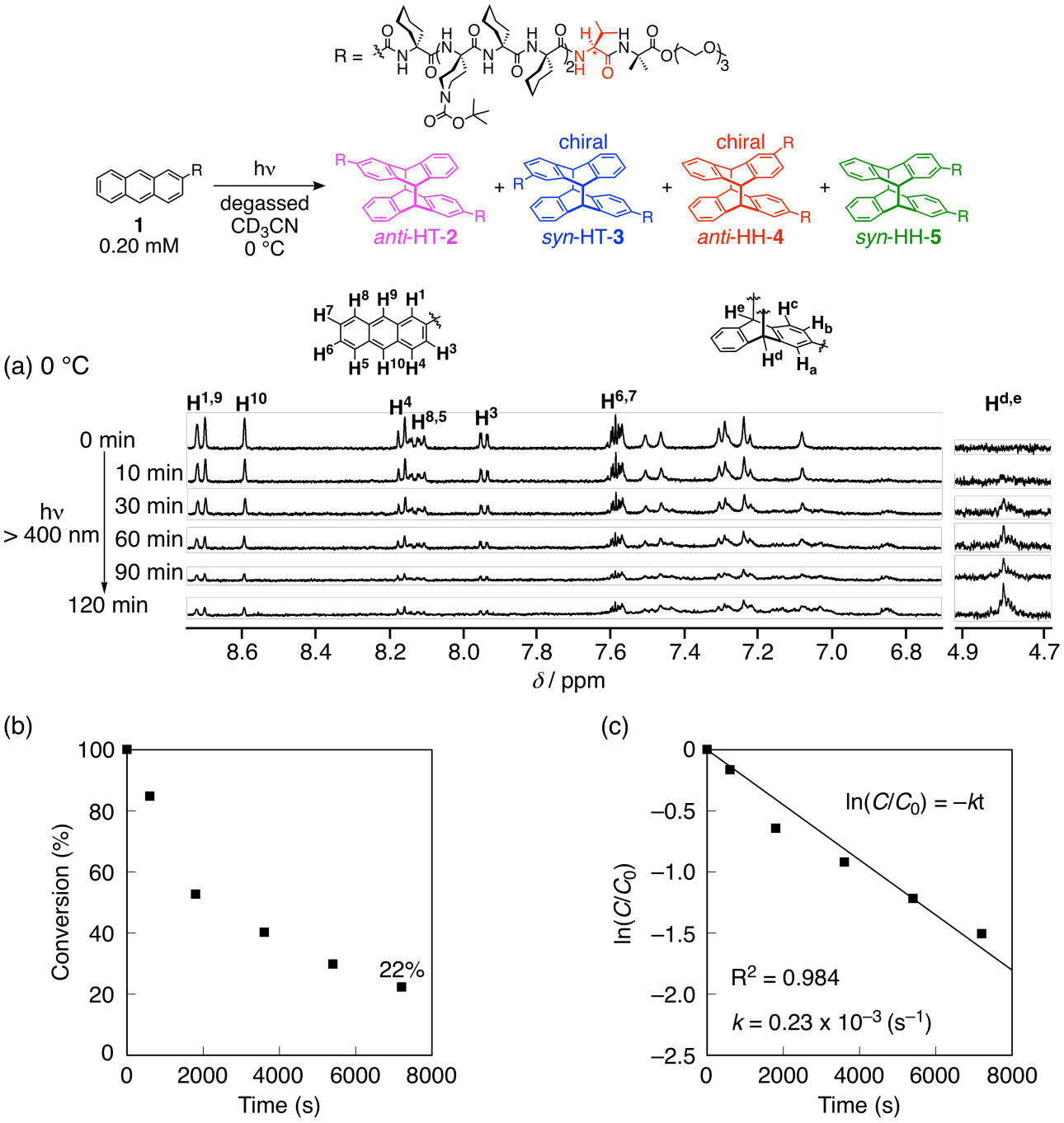

Fig. S6 (a) Time-dependent ^{1}H NMR spectral changes of **1** (500 MHz, degassed CD_3CN, 0.20 mM) upon light irradiation (> 400 nm) at 0 °C (run 3, Table 1) measured at 25 °C. The peak assignments of the anthracene unit were done on the basis of the *g*COSY and ROESY (Fig. S14) spectra measured in CD_3CN. (b,c) Time-conversion relationships (b) and kinetic plots (c) of the photodimerization of **1** (degassed CD_3CN, 0 °C, 0.20 mM) estimated from the integral ratios of the peaks for H^{10} (**1**) and 1,1,2,2-tetrachloroethane used as the internal standard on the basis of the ^{1}H NMR spectral changes shown in (a).

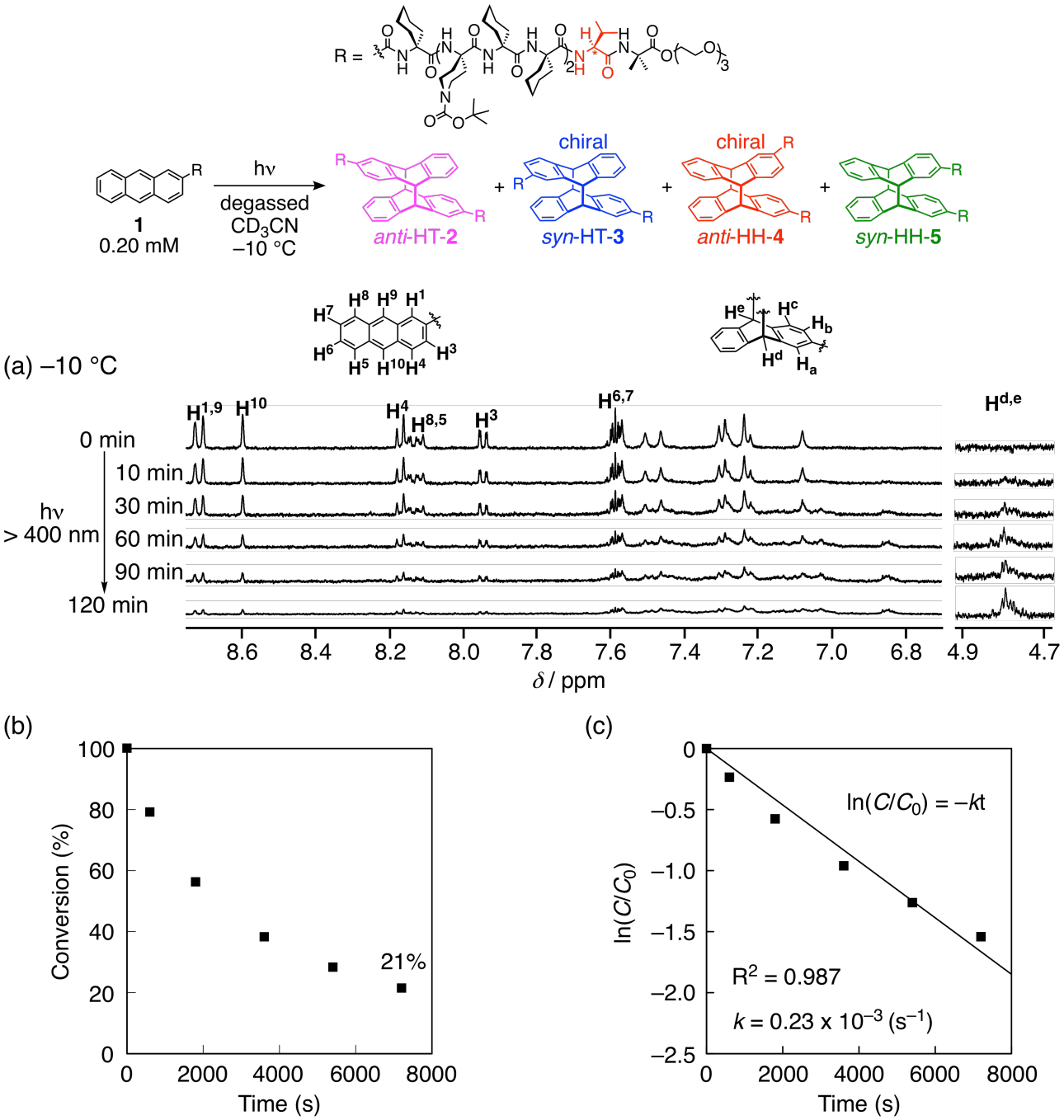

Fig. S7 (a) Time-dependent ^{1}H NMR spectral changes of **1** (500 MHz, degassed CD_3CN, 0.20 mM) upon light irradiation (> 400 nm) at –10 °C (run 4, Table 1) measured at 25 °C. The peak assignments of the anthracene unit were done on the basis of the *g*COSY and ROESY (Fig. S14) spectra measured in CD_3CN. (b,c) Time-conversion relationships (b) and kinetic plots (c) of the photodimerization of **1** (degassed CD_3CN, –10 °C, 0.20 mM) estimated from the integral ratios of the peaks for H^{10} (**1**) and 1,1,2,2-tetrachloroethane used as the internal standard on the basis of the ^{1}H NMR spectral changes shown in (a).

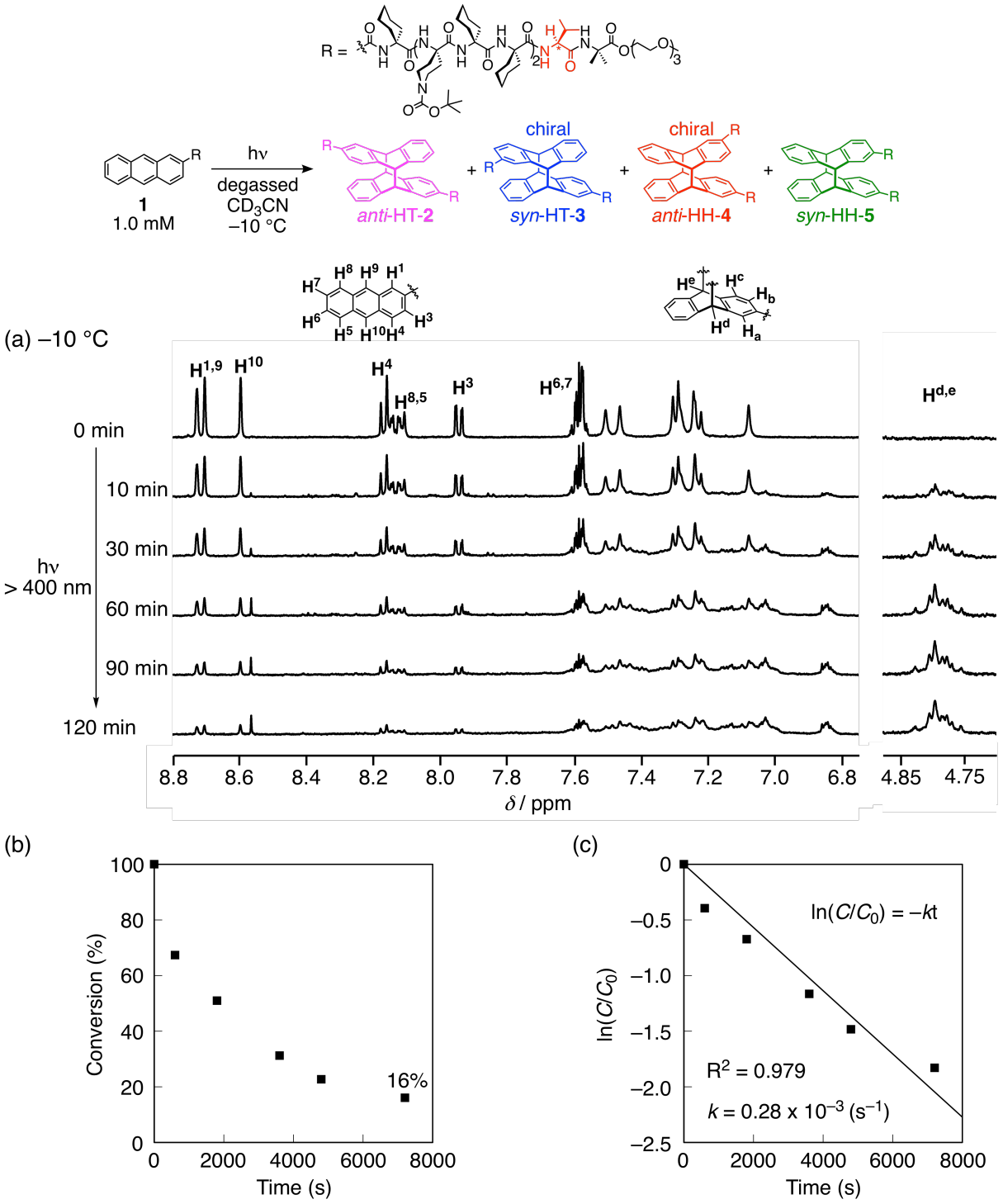

Fig. S8 (a) Time-dependent ^{1}H NMR spectral changes of **1** (500 MHz, degassed CD_3CN, 1.0 mM) upon light irradiation (> 400 nm) at –10 °C (run 5, Table 1) measured at 25 °C. The peak assignments of the anthracene unit were done on the basis of the *g*COSY and ROESY (Fig. S14) spectra measured in CD_3CN. (b,c) Time-conversion relationships (b) and kinetic plots (c) of the photodimerization of **1** (degassed CD_3CN, –10 °C, 1.0 mM) estimated from the integral ratios of the peaks for H^{10} (**1**) and 1,1,2,2-tetrachloroethane used as the internal standard on the basis of the ^{1}H NMR spectral changes shown in (a).

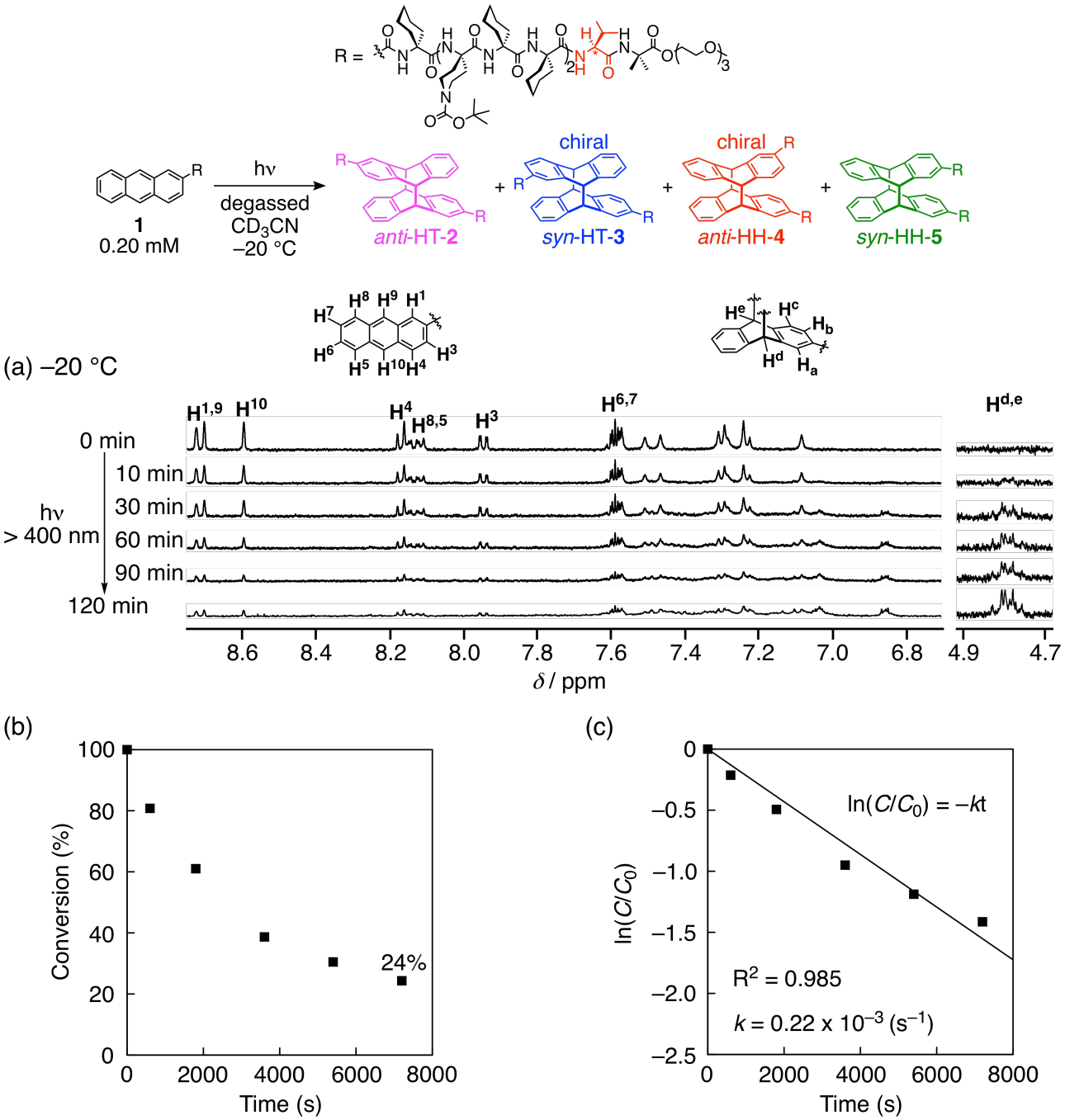

Fig. S9 (a) Time-dependent ^{1}H NMR spectral changes of **1** (500 MHz, degassed CD_3CN, 0.20 mM) upon light irradiation (> 400 nm) at –20 °C (run 6, Table 1) measured at 25 °C. The peak assignments of the anthracene unit were done on the basis of the *g*COSY and ROESY (Fig. S14) spectra measured in CD_3CN. (b,c) Time-conversion relationships (b) and kinetic plots (c) of the photodimerization of **1** (degassed CD_3CN, –20 °C, 0.20 mM) estimated from the integral ratios of the peaks for H^{10} (**1**) and 1,1,2,2-tetrachloroethane used as the internal standard on the basis of the ^{1}H NMR spectral changes shown in (a).

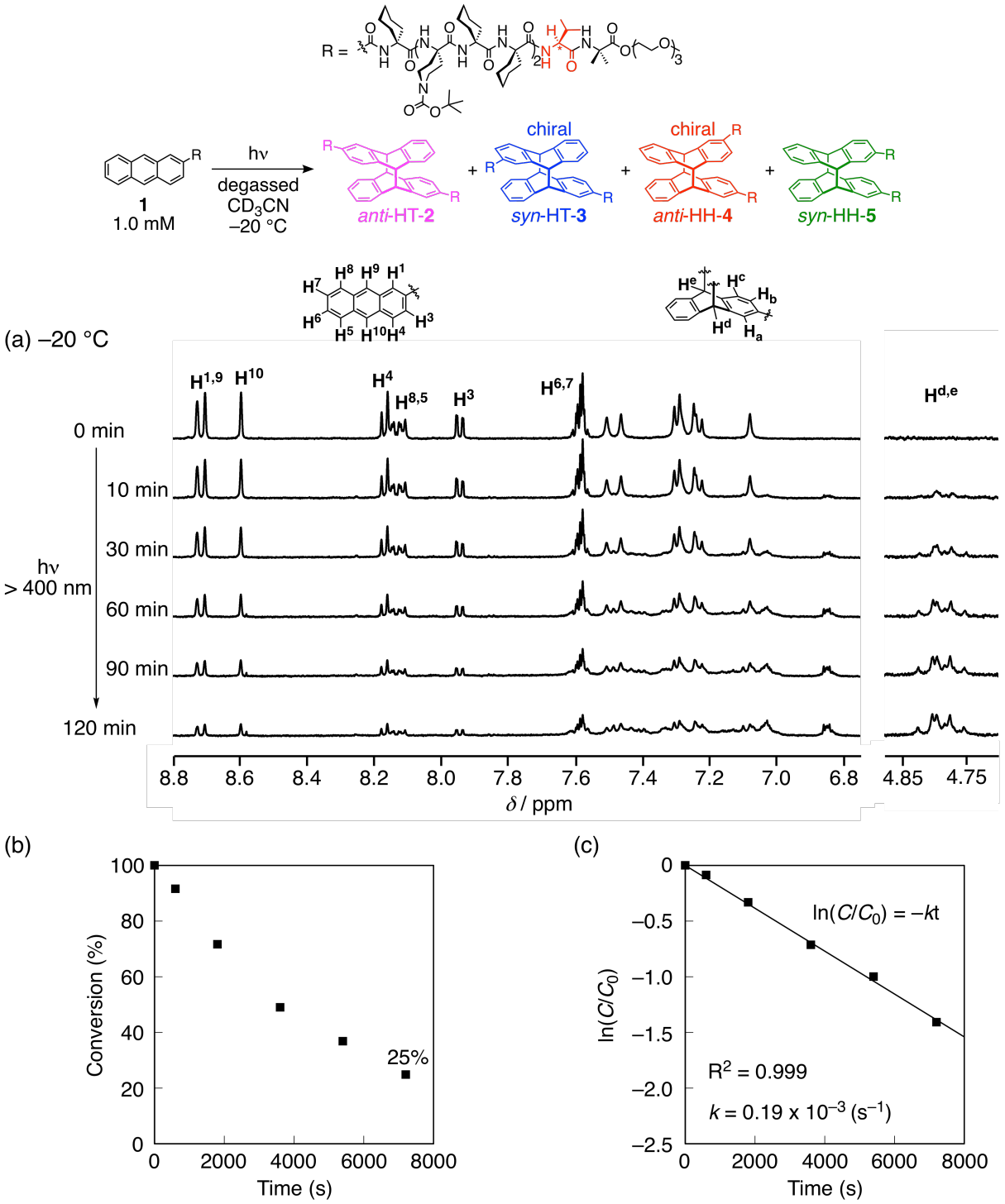

Fig. S10 (a) Time-dependent ^{1}H NMR spectral changes of **1** (500 MHz, degassed CD_3CN, 1.0 mM) upon light irradiation (> 400 nm) at –20 °C (run 7, Table 1) measured at 25 °C. The peak assignments of the anthracene unit were done on the basis of the *g*COSY and ROESY (Fig. S14) spectra measured in CD_3CN. (b,c) Time-conversion relationships (b) and kinetic plots (c) of the photodimerization of **1** (degassed CD_3CN, –20 °C, 1.0 mM) estimated from the integral ratios of the peaks for H^{10} (**1**) and 1,1,2,2-tetrachloroethane used as the internal standard on the basis of the ^{1}H NMR spectral changes shown in (a).

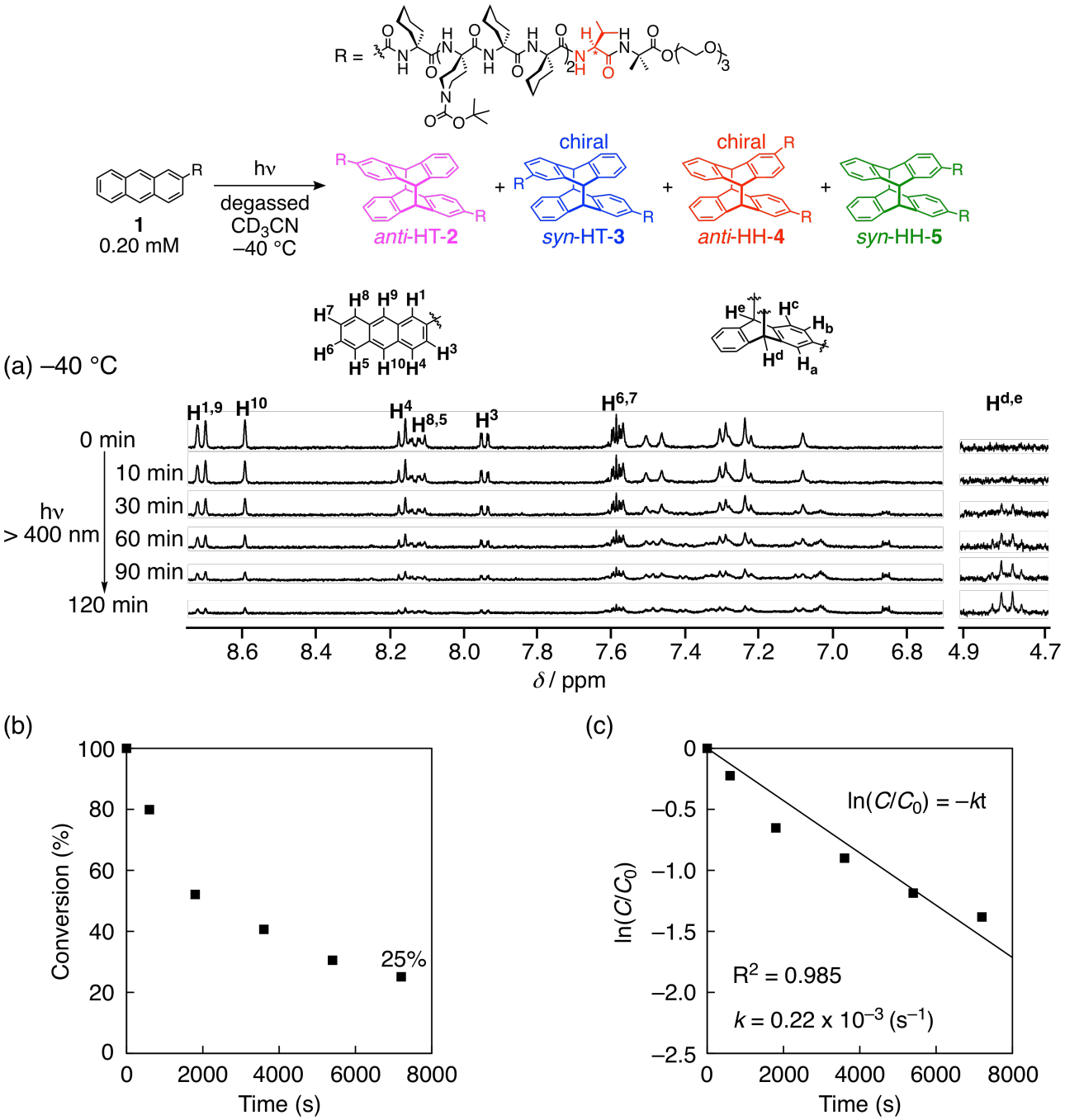

Fig. S11 (a) Time-dependent ^{1}H NMR spectral changes of **1** (500 MHz, degassed CD_3CN, 0.20 mM) upon light irradiation (> 400 nm) at –40 °C (run 8, Table 1) measured at 25 °C. The peak assignments of the anthracene unit were done on the basis of the *g*COSY and ROESY (Fig. S14) spectra measured in CD_3CN. (b,c) Time-conversion relationships (b) and kinetic plots (c) of the photodimerization of **1** (degassed CD_3CN, –40 °C, 0.20 mM) estimated from the integral ratios of the peaks for H^{10} (**1**) and 1,1,2,2-tetrachloroethane used as the internal standard on the basis of the ^{1}H NMR spectral changes shown in (a).

6-2. Determination of Relative Yields of Photodimers and Diastereomeric Excesses of Chiral *syn*-Photodimers Obtained by Photodimerization of 1 under Various Conditions and Plots of the Natural Logarithms of the HT/HH and Diastereomeric Ratios against the Reciprocal Temperature.

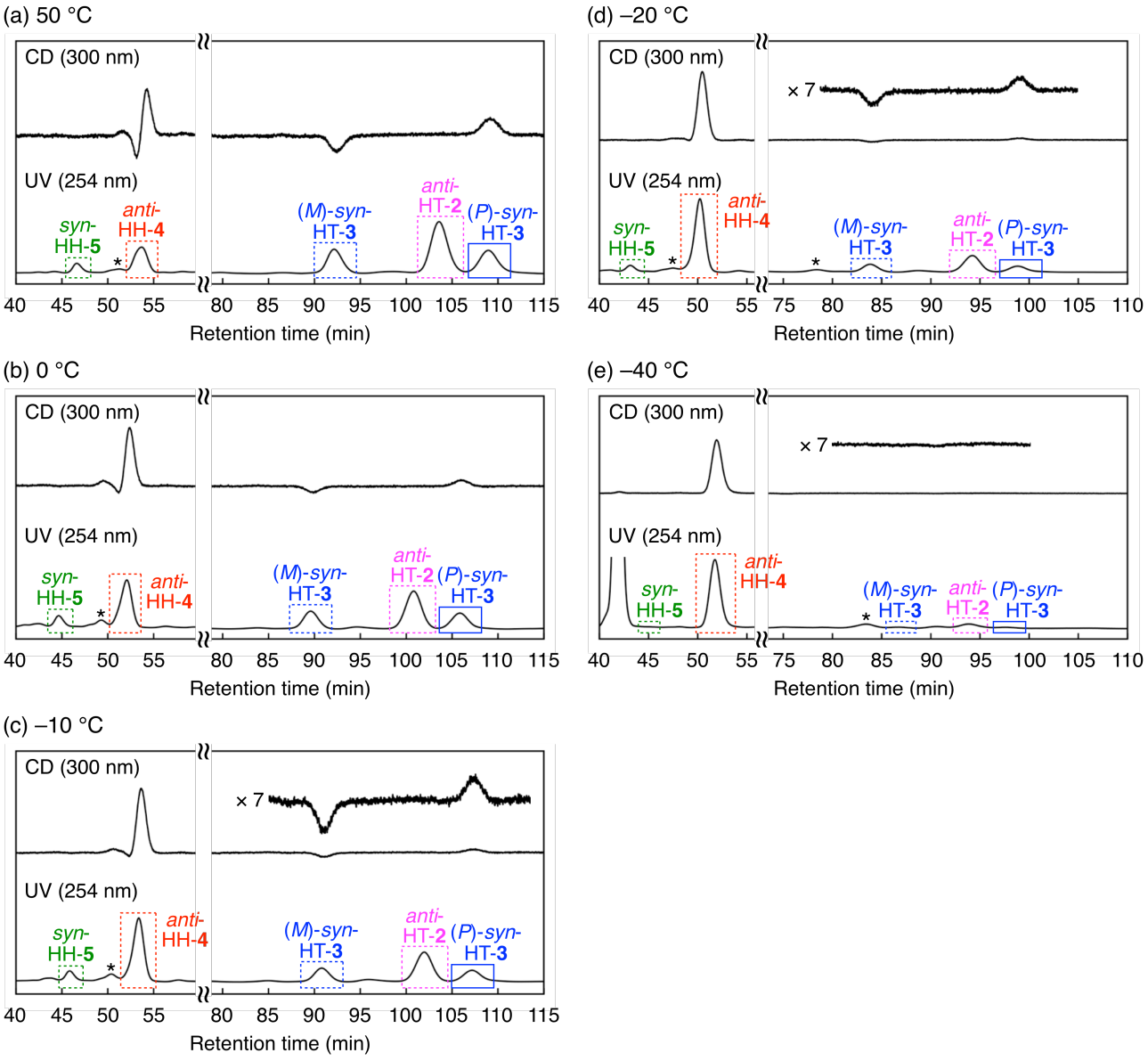

(Fig. S12 to be continued)

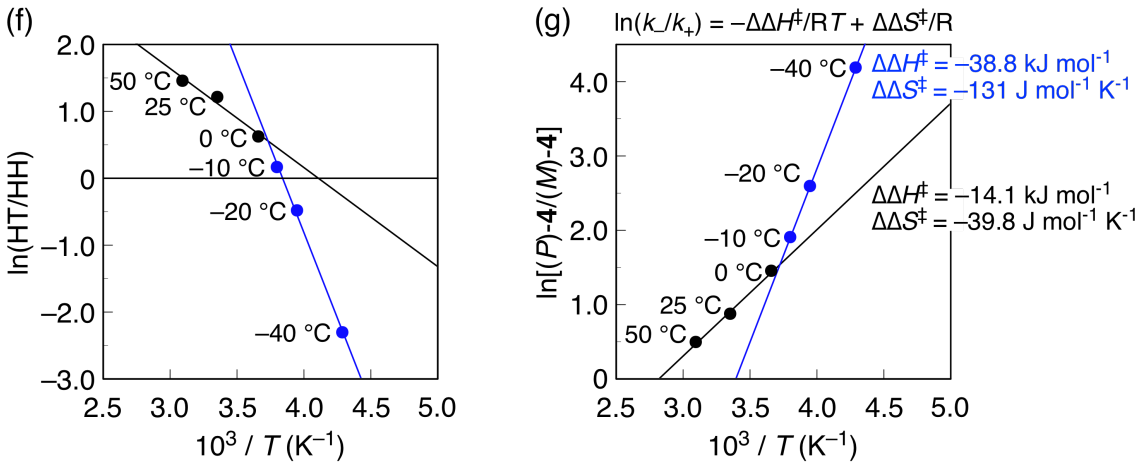

Fig. S12 (a–e) UV and CD detected HPLC chromatograms of photodimers obtained after light irradiation (> 400 nm) of **1** (0.20 mM) in degassed CD_3CN at 50 (a), 0 (b), –10 (c), –20 (d) and –40 °C (e) (runs 1, 3, 4, 6 and 8, Table 1). For the HPLC separation of the *anti*-HH-**4** diastereomers, see Fig. 3b. * denotes unknown impurities. (f,g) Plots of the natural logarithms of the HT/HH ratio of *anti*-HT-**2**, *syn*-HT-**3**, *anti*-HH-**4** and *syn*-HH-**5** (f) and the diastereomeric ratio of (*P*)- and (*M*)-*anti*-HH-**4** ([(*P*)-**4**]/[(*M*)-**4**]) (g) against the reciprocal temperature upon photoirradiation of **1** (data are taken from runs 1–4, 6 and 8, Table 1).

The thermodynamic parameters ($\Delta\Delta H^{\ddagger}$ and $\Delta\Delta S^{\ddagger}$) for the temperature-dependent diastereoselective photodimerization of **1** (Fig. S12g) were calculated from the slope and intercept of the plots showing two straight lines (Fig. 3d) based on the differential Eyring equation to be –14.1 kJ mol^{-1} and –39.8 J mol^{-1} K^{-1} for high-temperature region (50 – 0 °C) and –38.8 kJ mol^{-1} and –131 J mol^{-1} K^{-1} for low-temperature region (–10 – –40 °C), respectively. The same negative but different $\Delta\Delta H^{\ddagger}$ and $\Delta\Delta S^{\ddagger}$ values indicated that the predominant formation of the (*P*)-(+)-*anti*-HH-**4** diastereomer is enthalpically more favored at lower temperatures probably due to the better intermolecular hydrogen-bonding and/or hydrophobic interactions between the peptide chains and stacking interactions between the terminal anthracene linkers of **1** assisted by a chiral aggregate formation at low temperatures, which, on the other hand, causes a formation of entropically less favored supramolecular aggregates.

7. ROESY NMR Spectrum of 1.

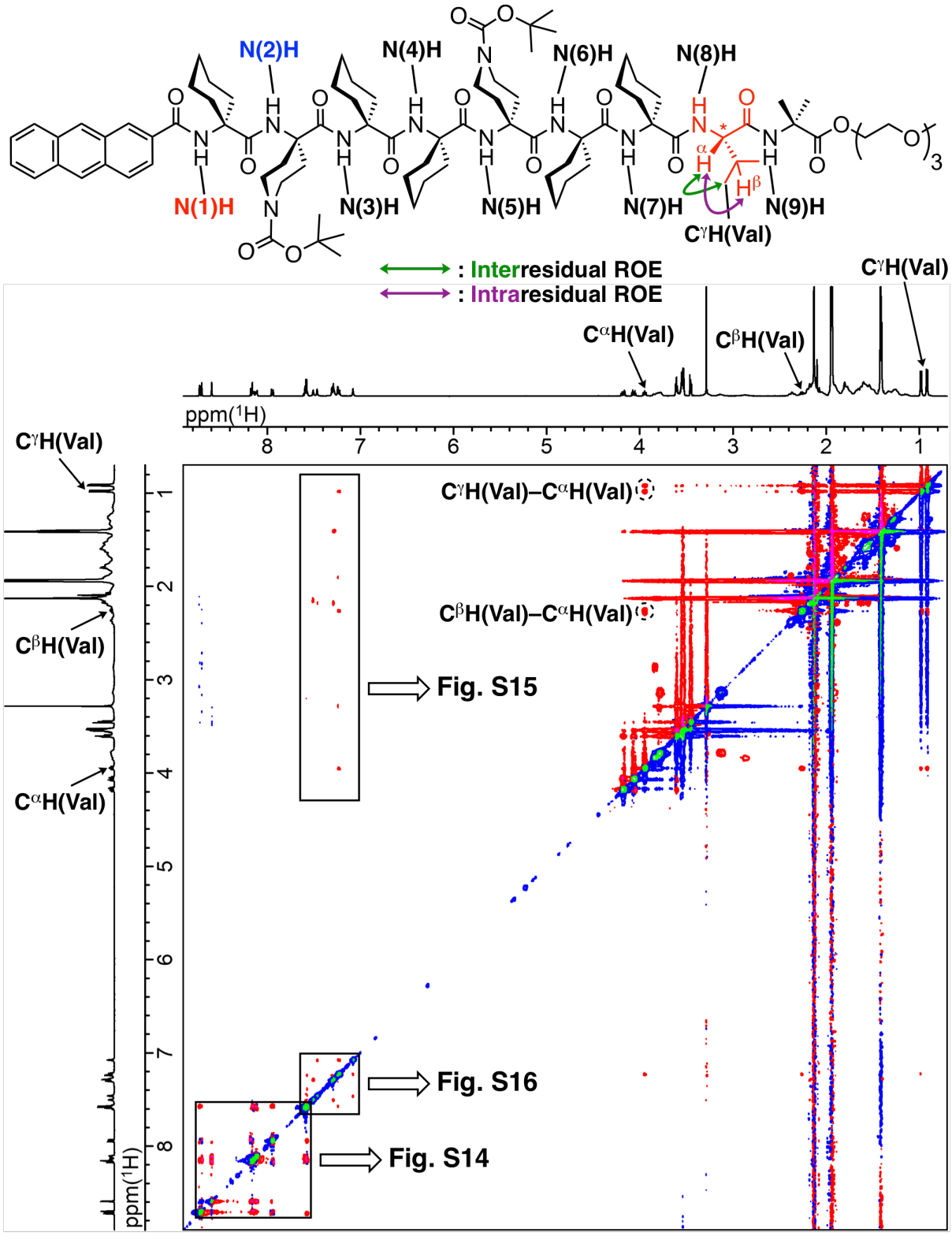

Fig. S13 ROESY spectrum of **1** (500 MHz, CD_3CN, 25.5 °C, 1.0 mM, mixing time = 500 ms).

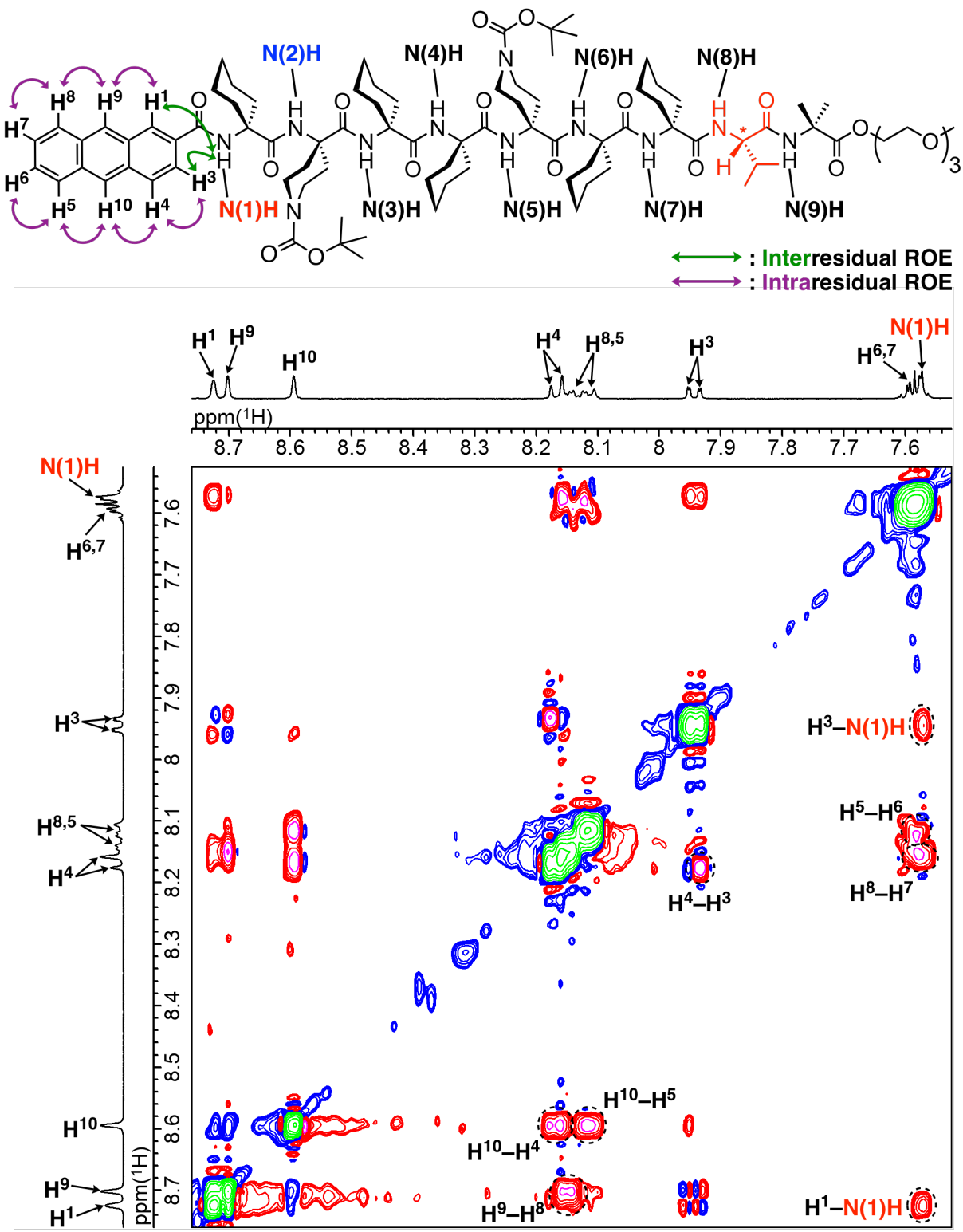

Fig. S14 Partial ROESY spectrum of **1** (500 MHz, CD_3CN, 25.5 °C, 1.0 mM, mixing time = 500 ms).

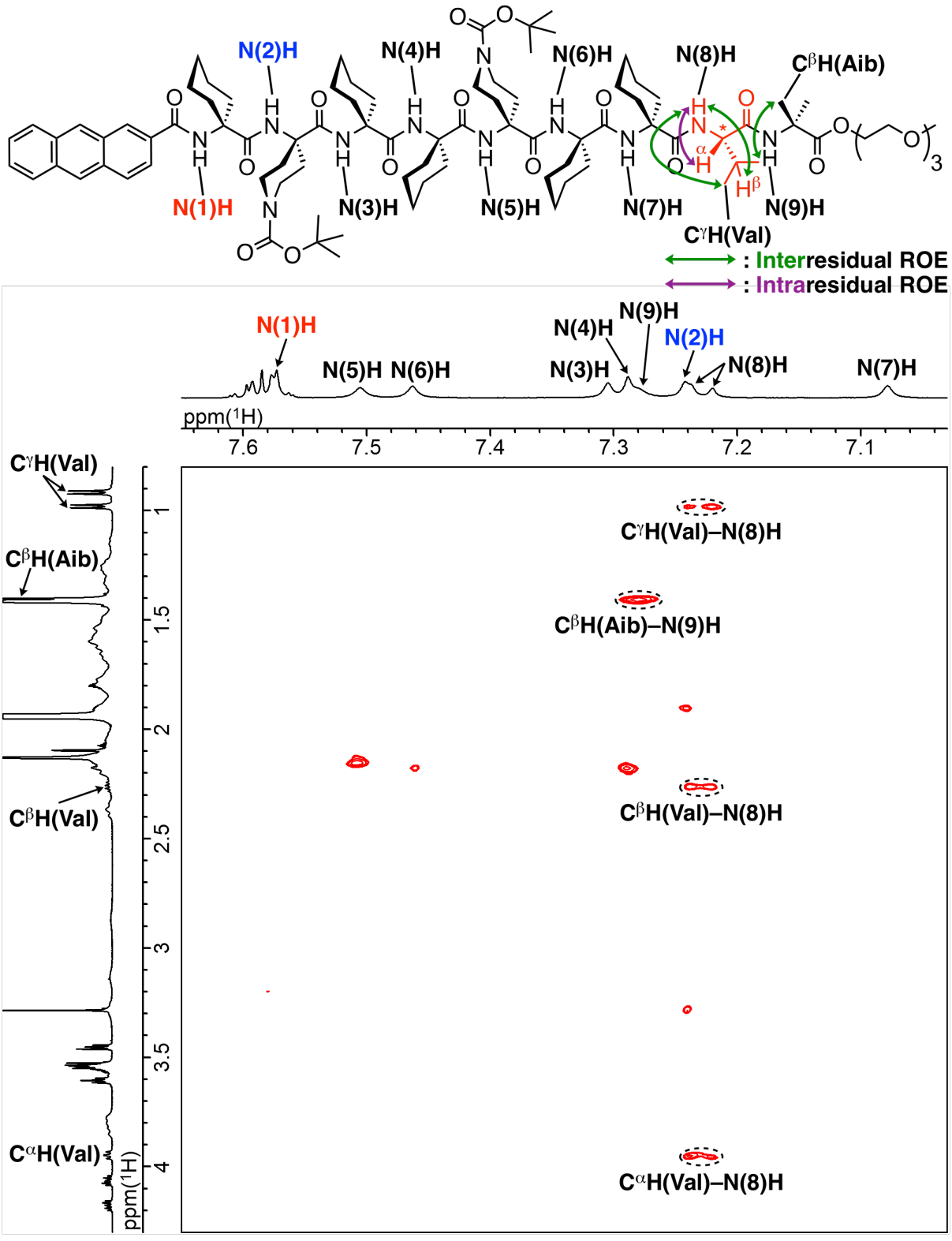

Fig. S15 Partial ROESY spectrum of **1** (500 MHz, CD_3CN, 25.5 °C, 1.0 mM, mixing time = 500 ms).

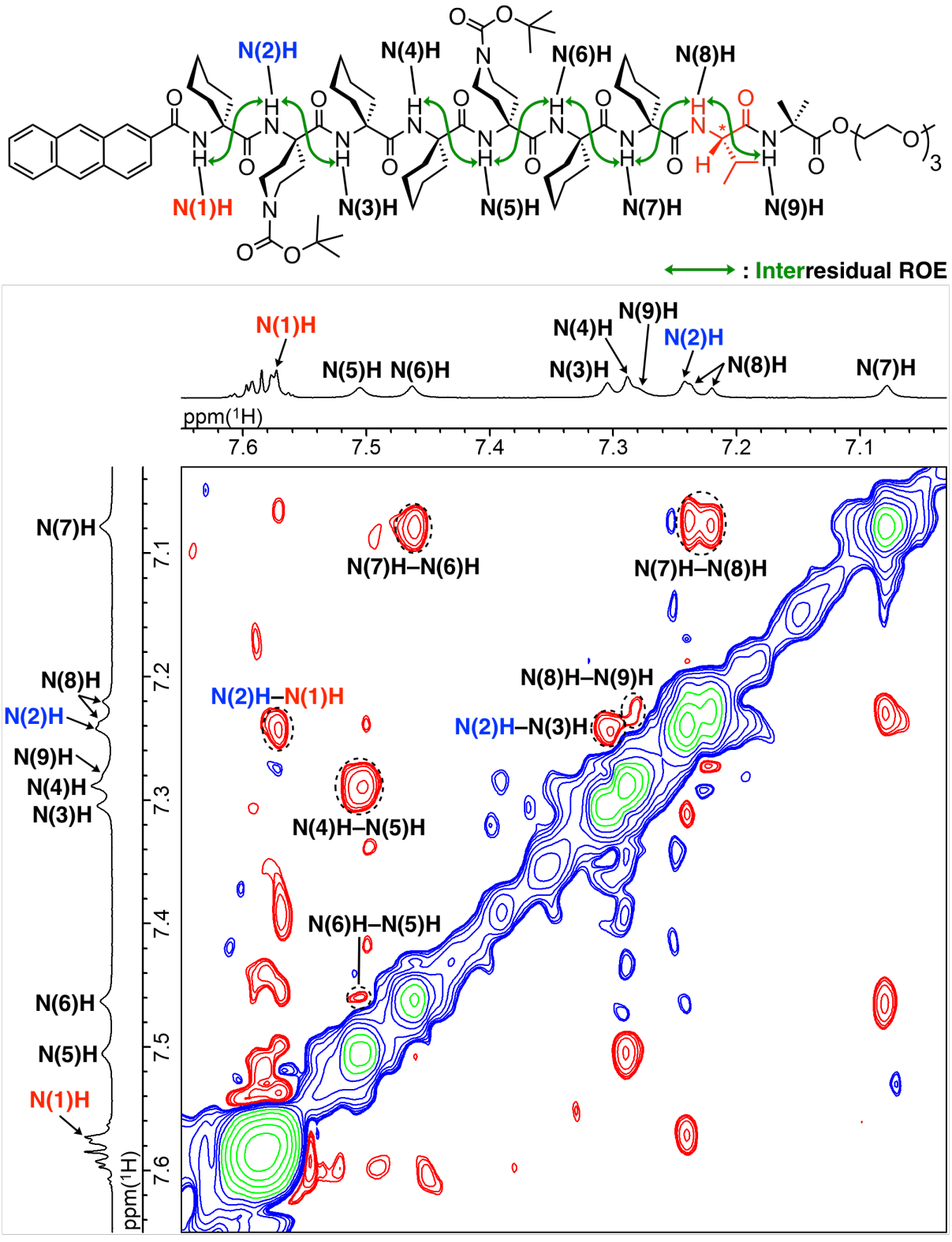

Fig. S16 Partial ROESY spectrum of **1** (500 MHz, CD_3CN, 25.5 °C, 1.0 mM, mixing time = 500 ms).

8. Concentration- and Temperature-Dependent ^{1}H NMR Spectral Changes.

8-1. Concentration-Dependent ^{1}H NMR Spectral Changes of 1 in CD_3CN.

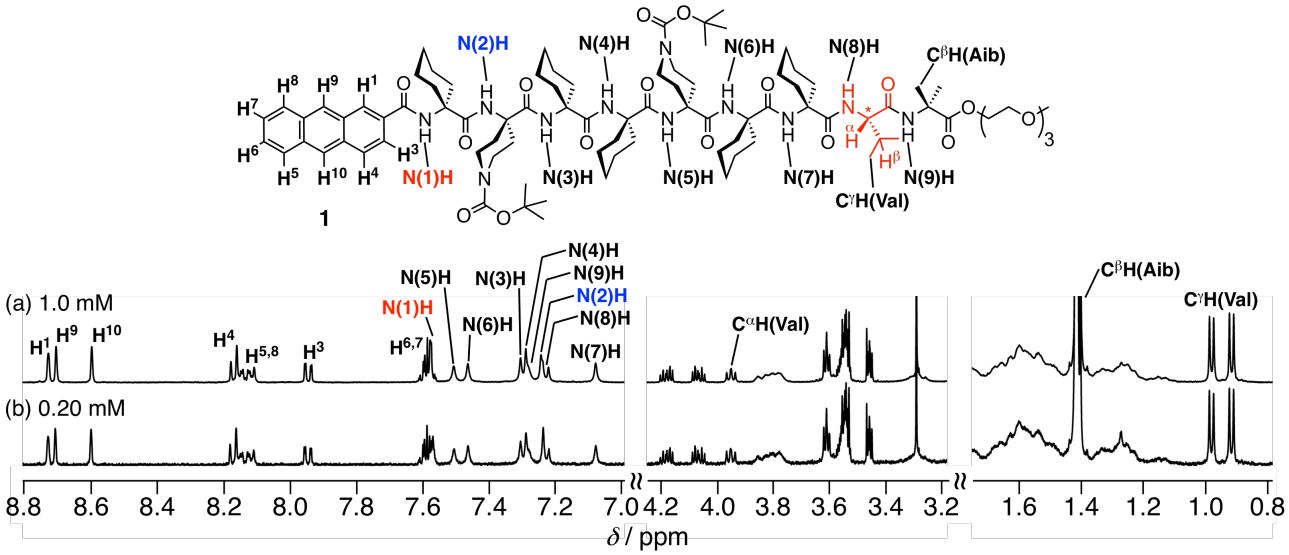

Fig. S17 ^{1}H NMR spectra of **1** (500 MHz, CD_3CN, 25 °C, 1.0 (a) and 0.20 mM (b)).

8-2. Temperature-Dependent ^{1}H NMR Spectral Changes of 1 and 6 in CD_3CN.

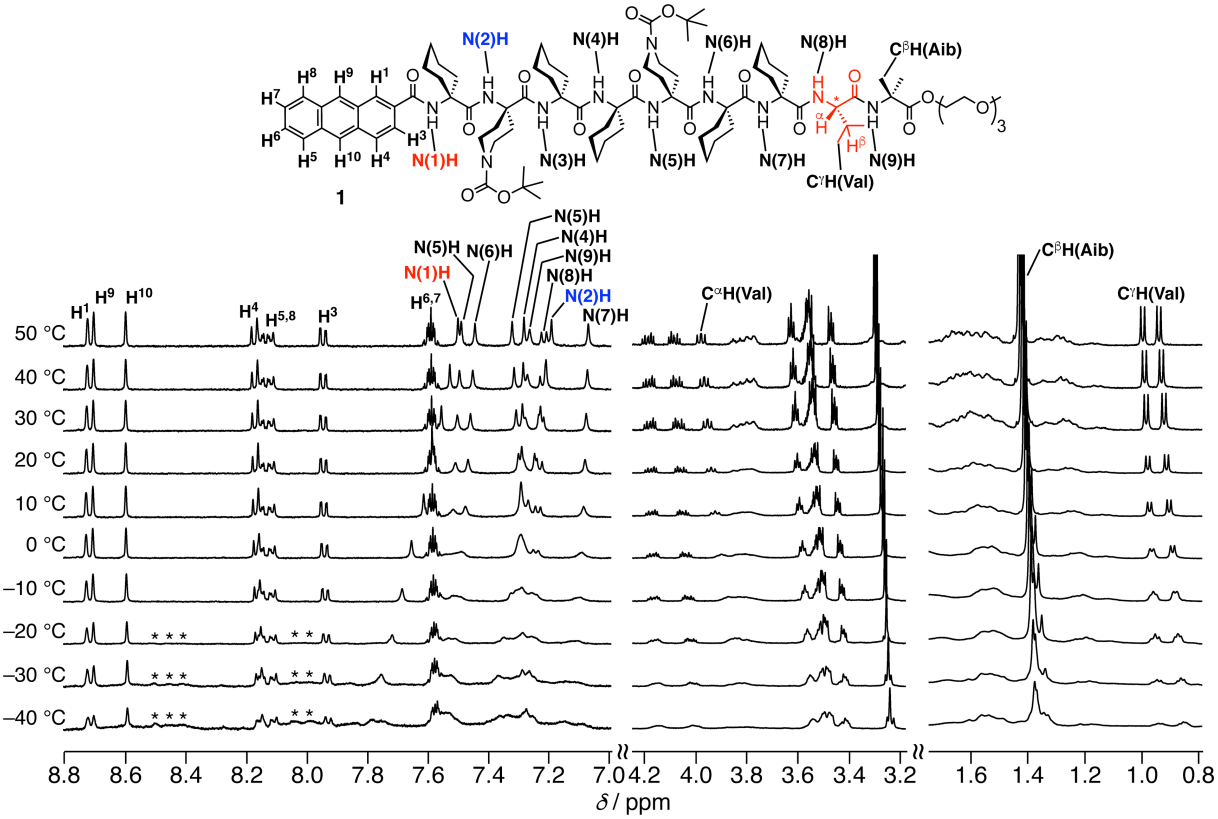

Fig. S18 Temperature-dependent ^{1}H NMR spectral changes of **1** (500 MHz, CD_3CN, 0.20 mM). * denotes the peaks probably due to the aggregate formation. The anthracene protons (H^1–H^{10}) together with the amide protons in the nonapeptide chain were assigned based on the 2D *g*COSY and ROESY (Figs. S13–S16) spectra of **1** (1.0 mM) in CD_3CN at 25 °C. * denotes the aromatic protons of the anthracene unit of **1** appeared at low temperatures.

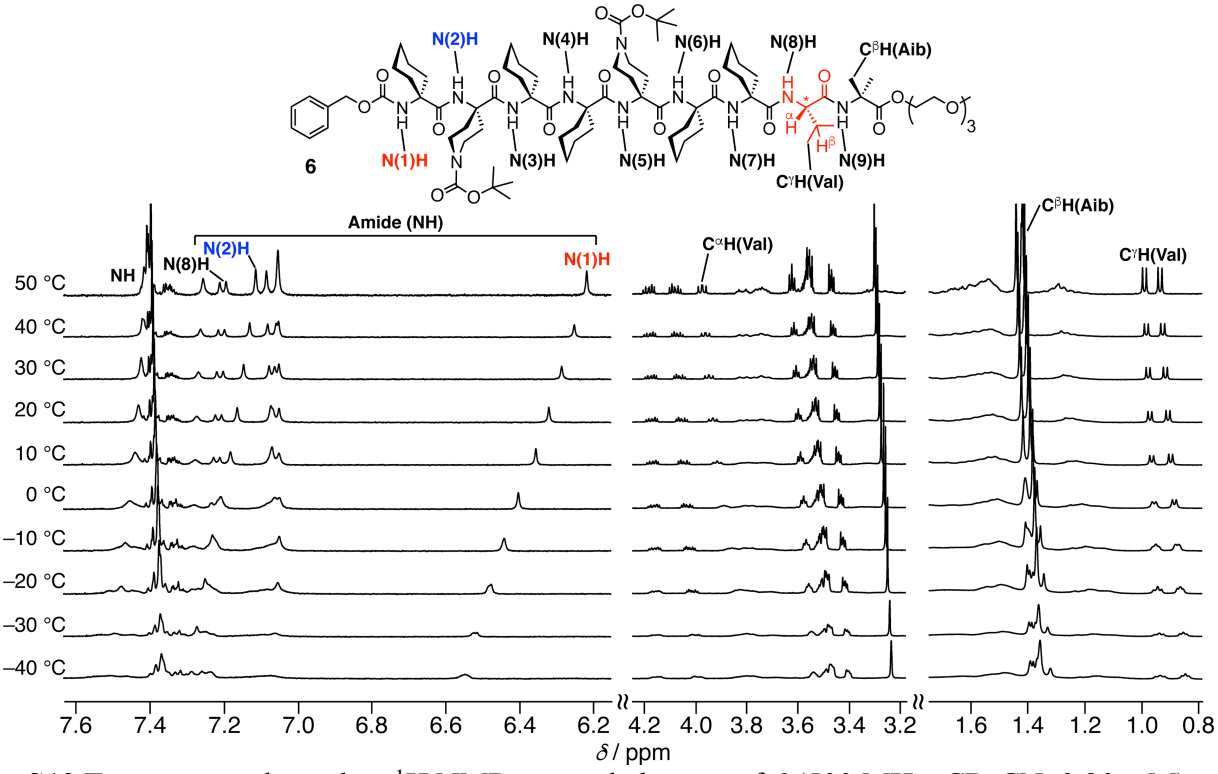

Fig. S19 Temperature-dependent ^{1}H NMR spectral changes of **6** (500 MHz, CD_3CN, 0.20 mM).

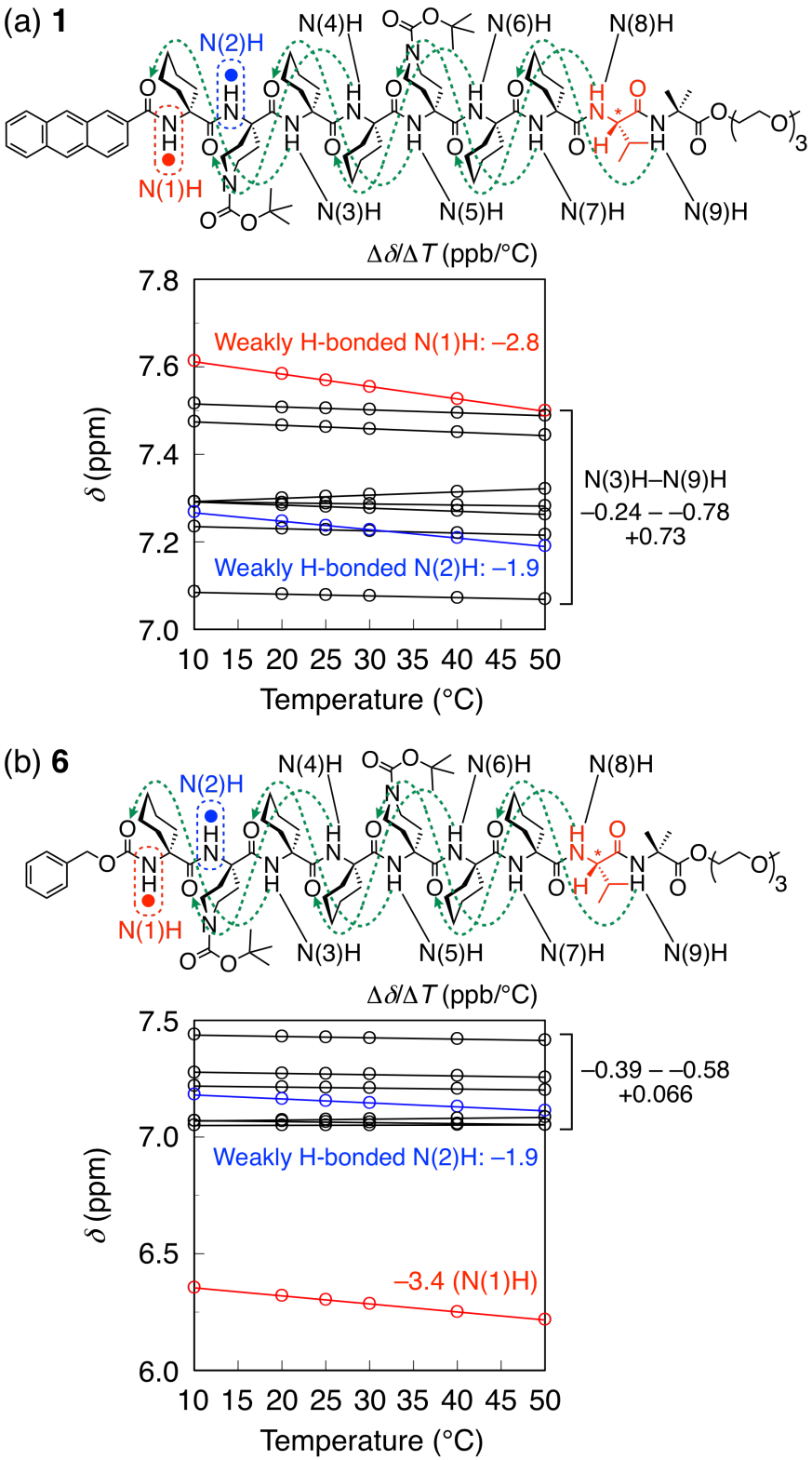

Fig. S20 Plots of the NH chemical shifts in the ^{1}H NMR spectra (Figs. S18 and S19) as a function of temperature in CD_3CN for **1** (0.20 mM) (a) and **6** (0.20 mM) (b). The amide NH temperature coefficients ($\Delta\delta/\Delta T$, ppb/°C) are also shown. On the basis of the $\Delta\delta/\Delta T$ values of **1**, the N(1)H and N(2)H protons of **1** are weakly solvated with CD_3CN and the other amide protons are involved in the hydrogen-bonded network to form the 3_{10}-helix, as supported by its ROESY spectrum (Figs. S15 and S16).[S5]

9. Comparison of the Cotton Effect Signs of Chiral *anti*- and *syn*-Photodimers with that of 1.

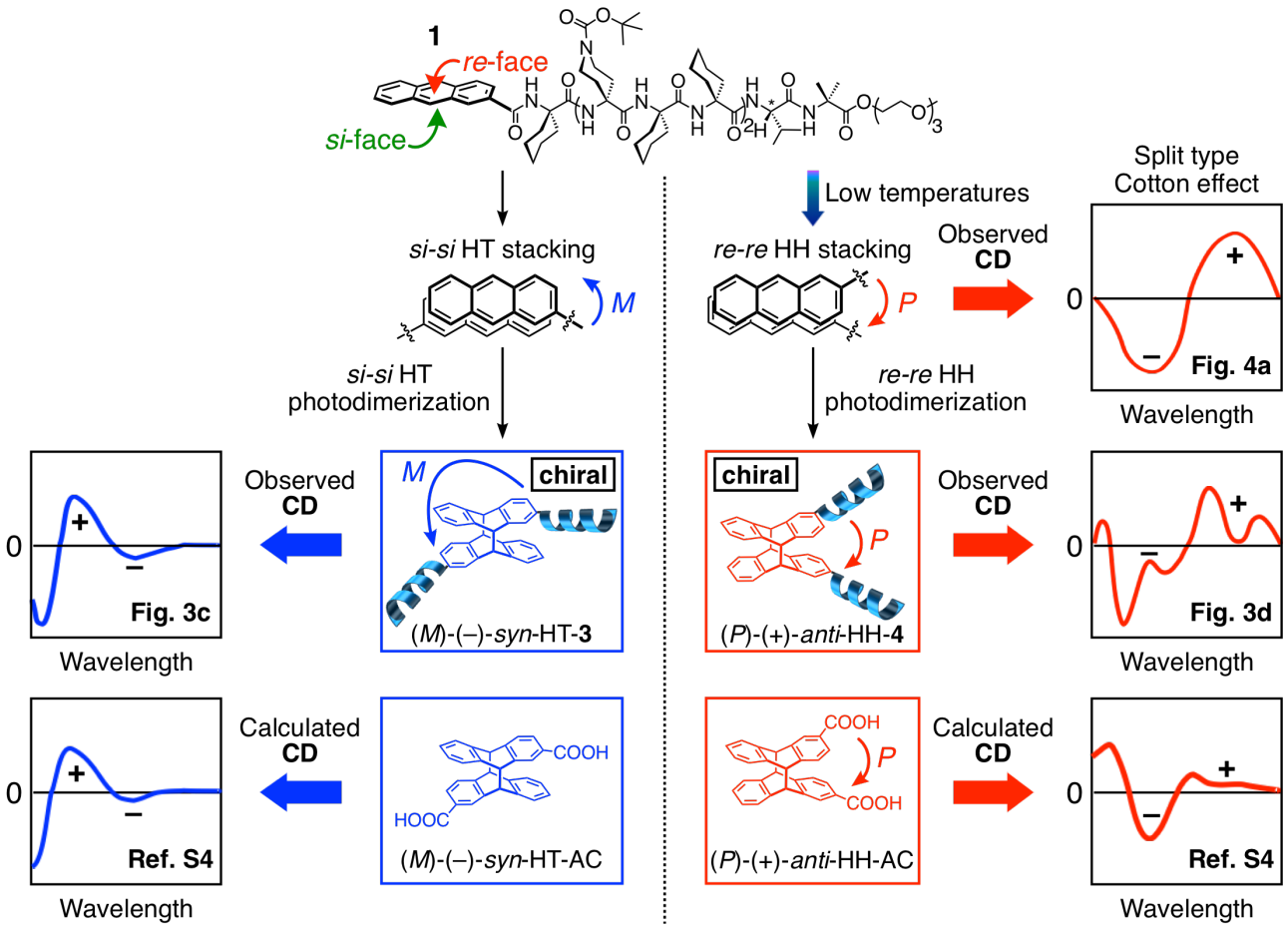

Fig. S21 Comparison of the Cotton effect signs of chiral *anti*- and *syn*-photodimers ((*P*)-*anti*-HH-**4** (right) and (*M*)-*syn*-HT-**3** (left)) with that of **1**. The positive-negative exciton-coupled Cotton effect of **1** at low temperatures suggests that the two anthracene units of **1** are arranged in a (*P*) *re-re*-stacked orientation (right, top). The (*P*)-*anti*-HH-**4** and (*M*)-*syn*-HT-**3** cyclophotodimers preferentially produced by photoirradiation of **1** at low temperatures also show positive-negative (right, middle) and negative-positive (left, middle) exciton-coupled Cotton effects, respectively, which are in good agreement with the calculated Cotton effects of the chiral *anti*- and *syn*-photodimers ((*P*)-*anti*-HH-AC (right, bottom) and (*M*)-*syn*-HT-AC (left, bottom)) of 2-anthracenecarboxylic acid (AC) reported by Inoue and co-workers.[S4]

10. Supporting References.

S1 C. L. Wysong, T. S. Yokum, G. A. Morales, R. L. Gundry, M. L. Mclaughlin and R. P. Hammer, *J. Org. Chem.*, 1996, **61**, 7650–7651.

S2 N. Ousaka, Y. Takeyama, H. Iida and E. Yashima, *Nat. Chem.*, 2011, **3**, 856–861.

S3 P. Tailleur and L. Berlinguet, *Can. J. Chem.*, 1961, **39**, 1309–1320.

S4 A. Wakai, H. Fukasawa, C. Yang, T. Mori and Y. Inoue, *J. Am. Chem. Soc.*, 2012, **134**, 4990–4997.

S5 (a) G. M. Bonora, C. Mapelli, C. Toniolo, R. R. Wilkening and E. S. Stevens, *Int. J. Biol. Macromol.*, 1984, **6**, 179–188; (b) A. Polese, F. Formaggio, M. Crisma, G. Valle, C. Toniolo, G. M. Bonora, Q. B. Broxterman and J. Kamphuis, *Chem. Eur. J.*, 1996, **2**, 1104–1111.

11. Spectroscopic Data.

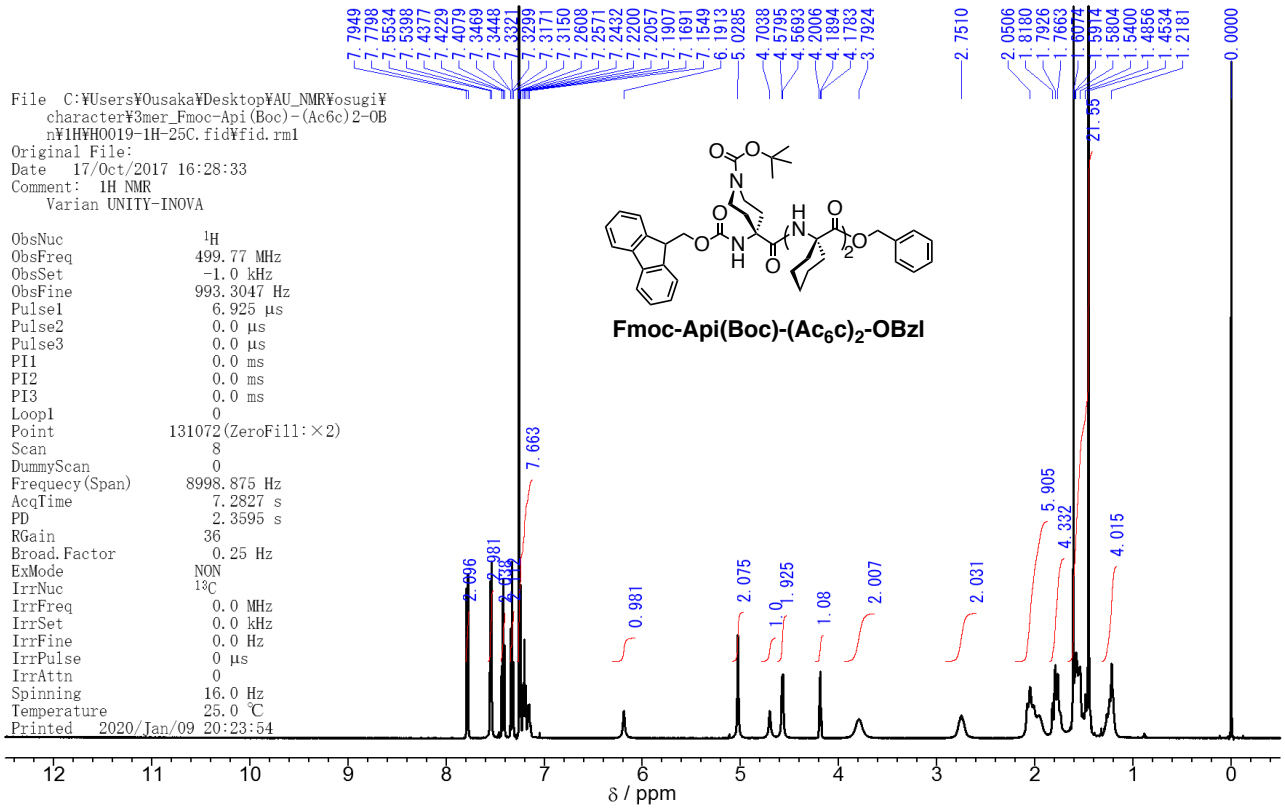

Fig. S22 ^{1}H NMR spectrum of Fmoc-Api(Boc)-(Ac$_6$c)$_2$-OBzl in $CDCl_3$ at 25 ºC.

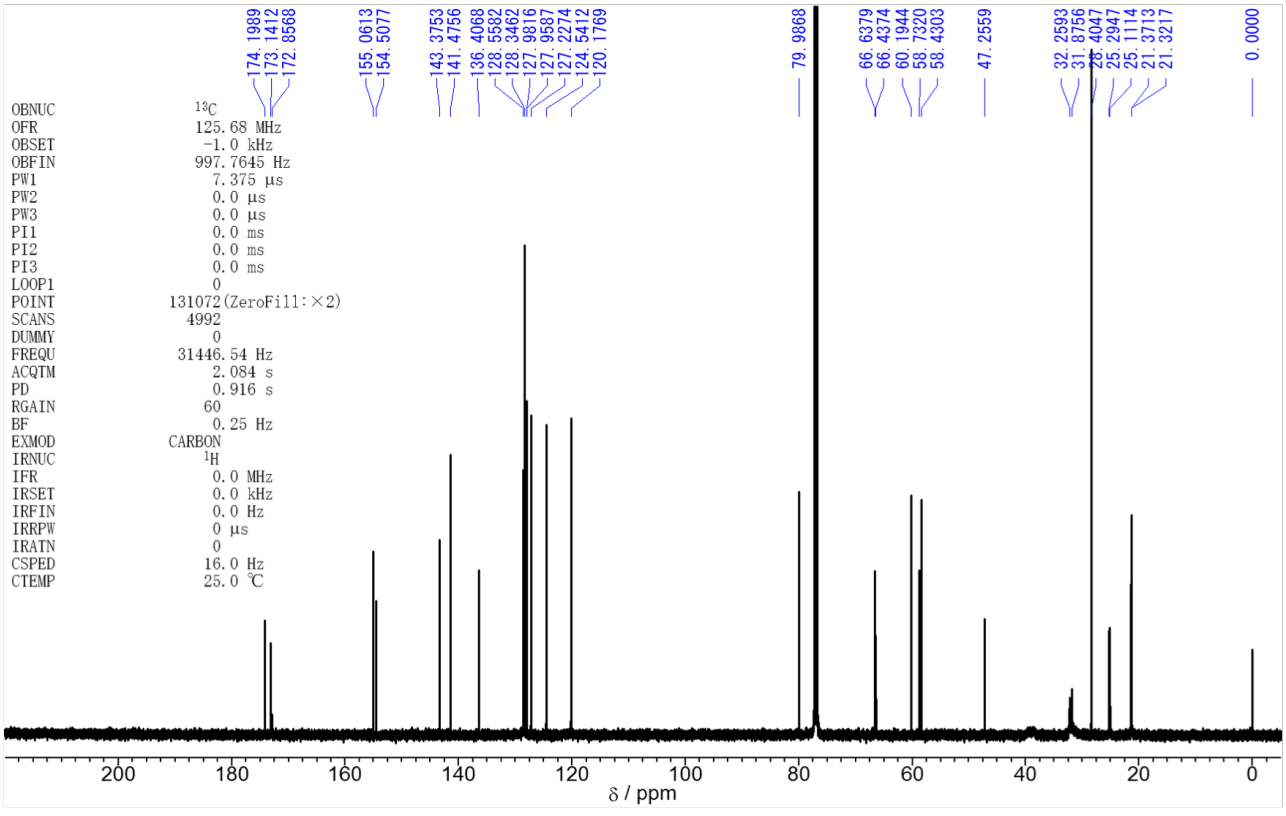

Fig. S23 ^{13}C NMR spectrum of Fmoc-Api(Boc)-(Ac$_6$c)$_2$-OBzl in $CDCl_3$ at 25 ºC.

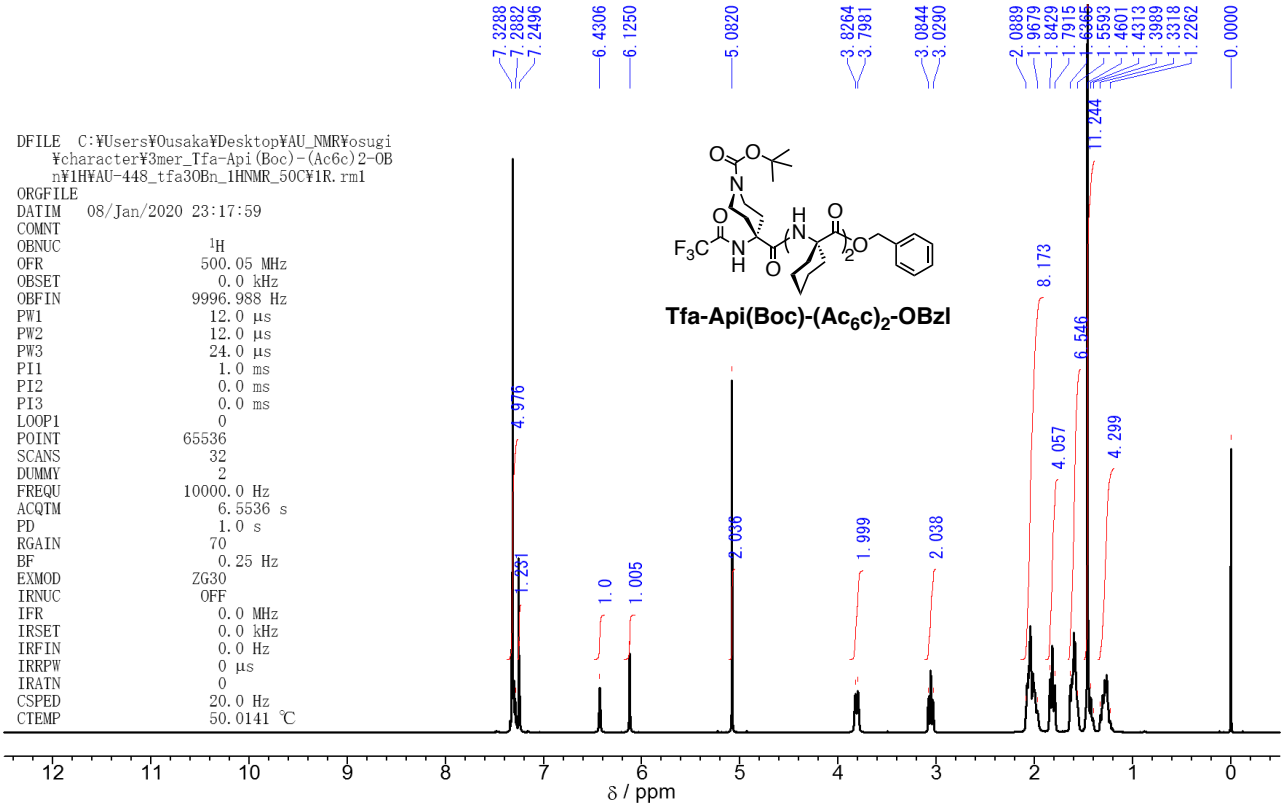

Fig. S24 ^{1}H NMR spectrum of Tfa-Api(Boc)-(Ac$_6$c)$_2$-OBzl in $CDCl_3$ at 50 ºC.

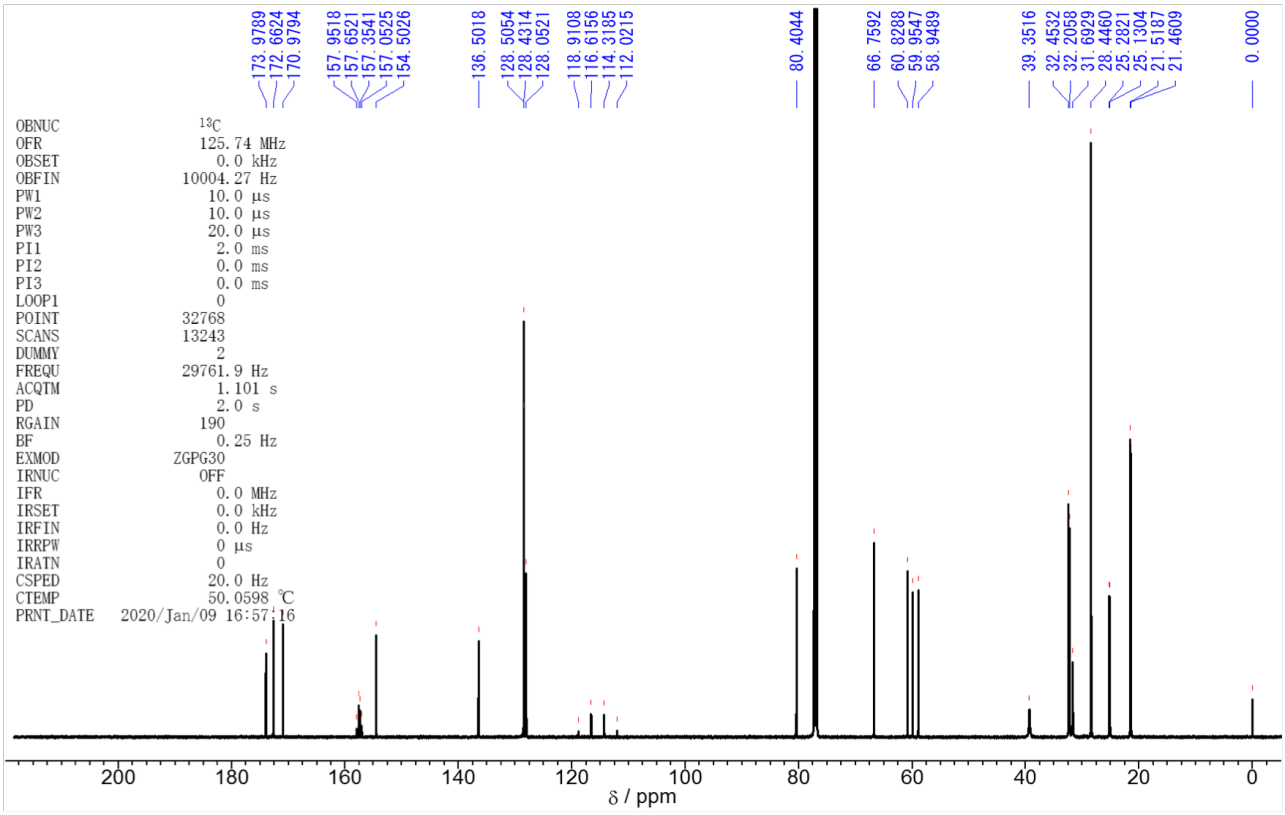

Fig. S25 ^{13}C NMR spectrum of Tfa-Api(Boc)-(Ac$_6$c)$_2$-OBzl in $CDCl_3$ at 50 ºC.

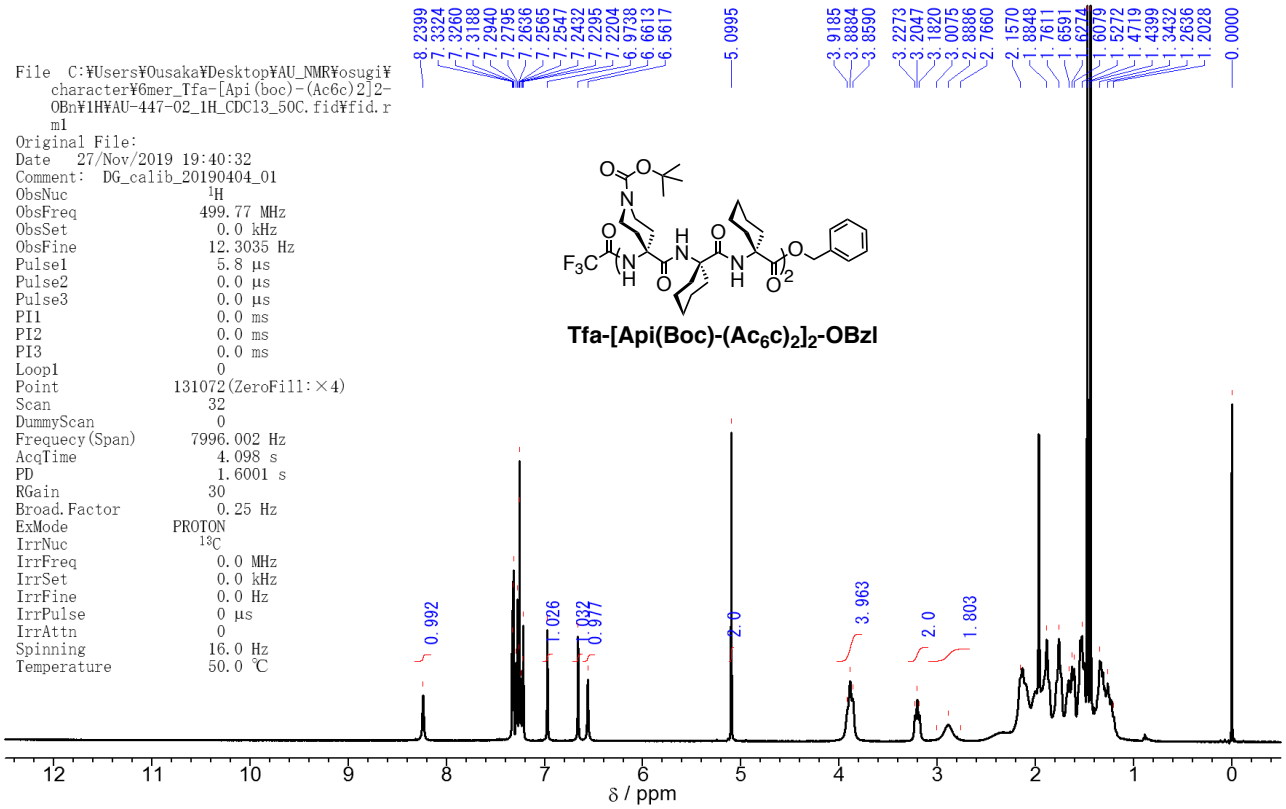

Fig. S26 ^{1}H NMR spectrum of Tfa-[Api(Boc)-(Ac$_6$c)$_2$]$_2$-OBzl in $CDCl_3$ at 50 ºC.

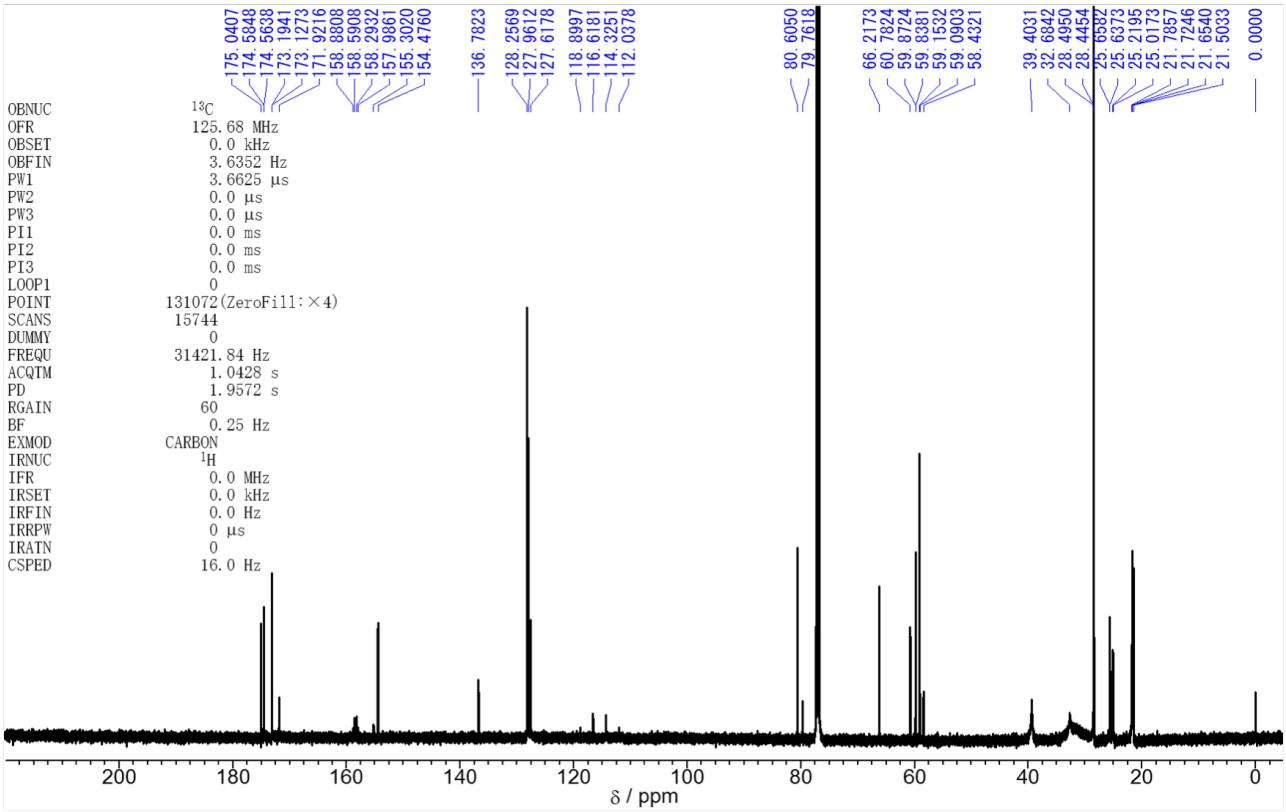

Fig. S27 ^{13}C NMR spectrum of Tfa-[Api(Boc)-(Ac$_6$c)$_2$]$_2$-OBzl in $CDCl_3$ at 50 ºC.

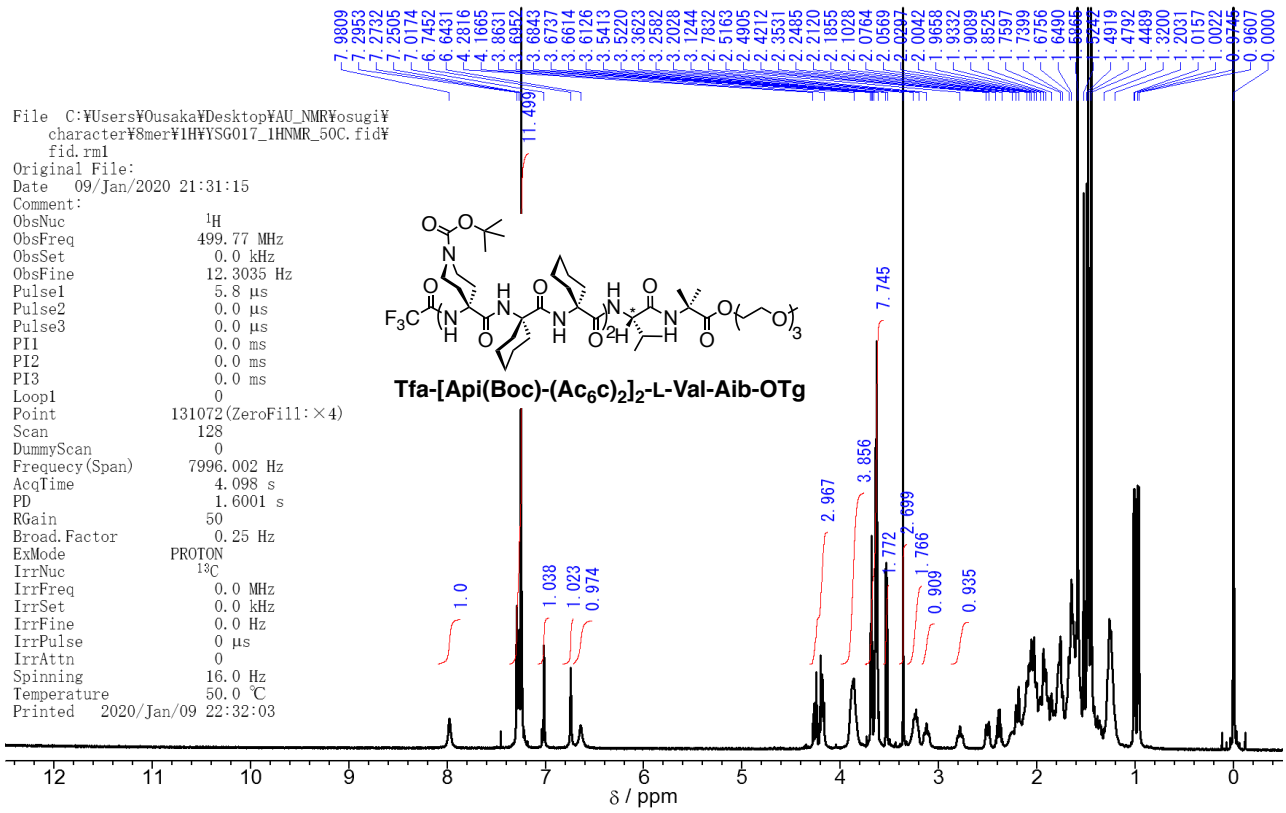

Fig. S28 ^{1}H NMR spectrum of Tfa-[Api(Boc)-(Ac$_6$c)$_2$]$_2$-L-Val-Aib-OTg in $CDCl_3$ at 50 ºC.

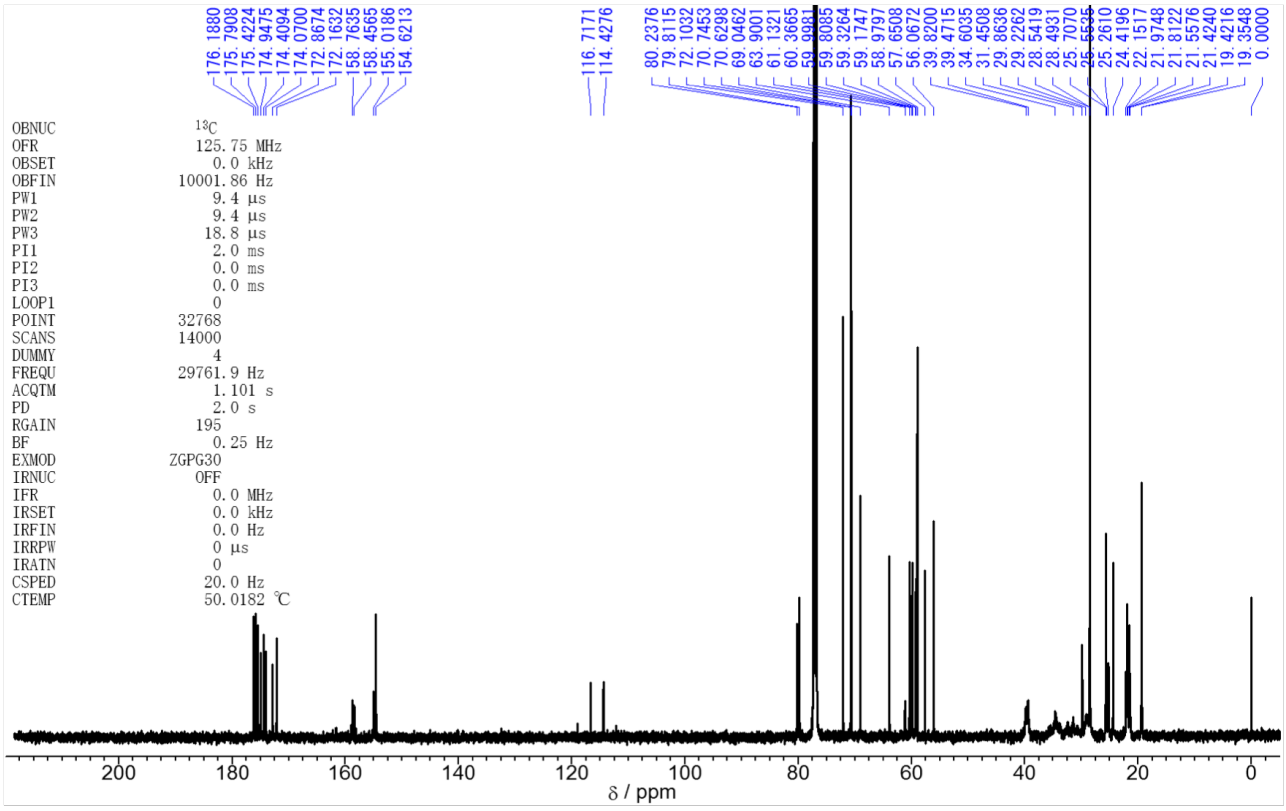

Fig. S29 ^{13}C NMR spectrum of Tfa-[Api(Boc)-(Ac$_6$c)$_2$]$_2$-L-Val-Aib-OTg in $CDCl_3$ at 50 ºC.

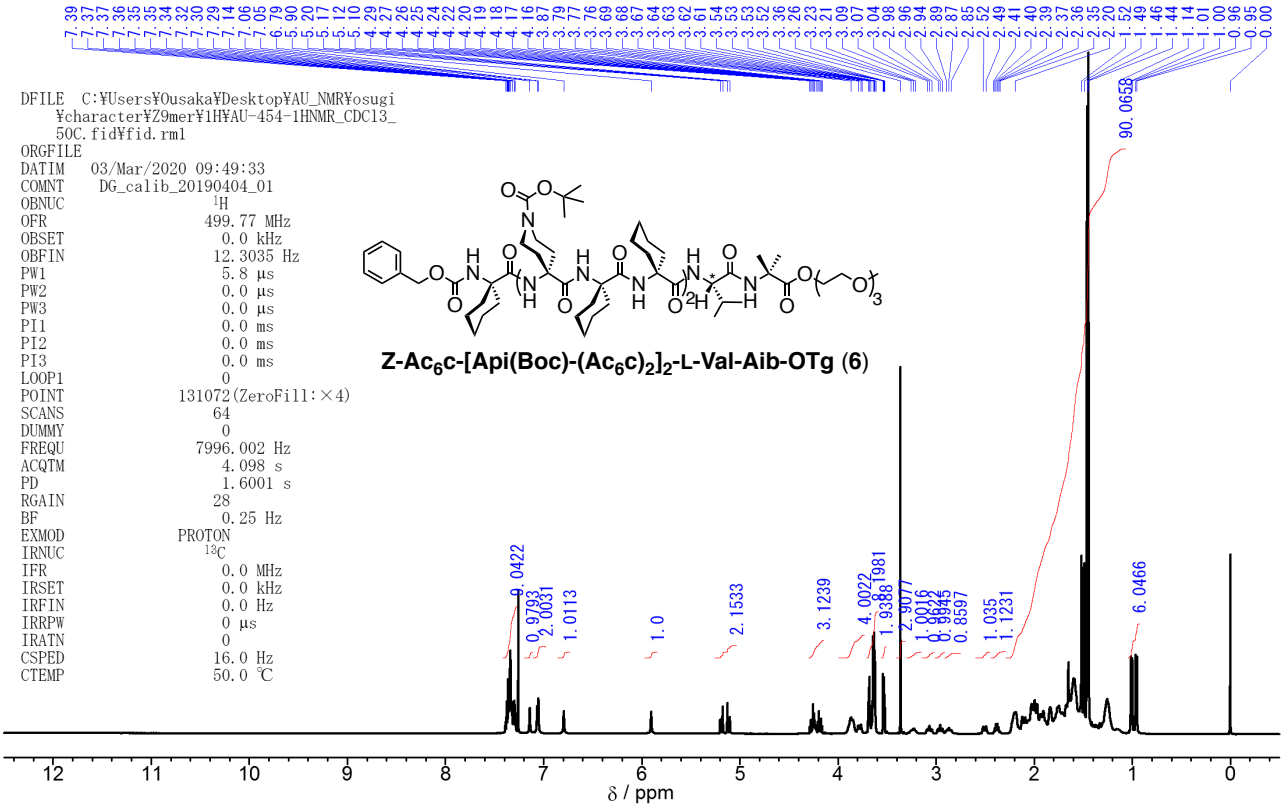

Fig. S30 ^{1}H NMR spectrum of Z-Ac$_6$c-[Api(Boc)-(Ac$_6$c)$_2$]$_2$-L-Val-Aib-OTg (**6**) in $CDCl_3$ at 50 ºC.

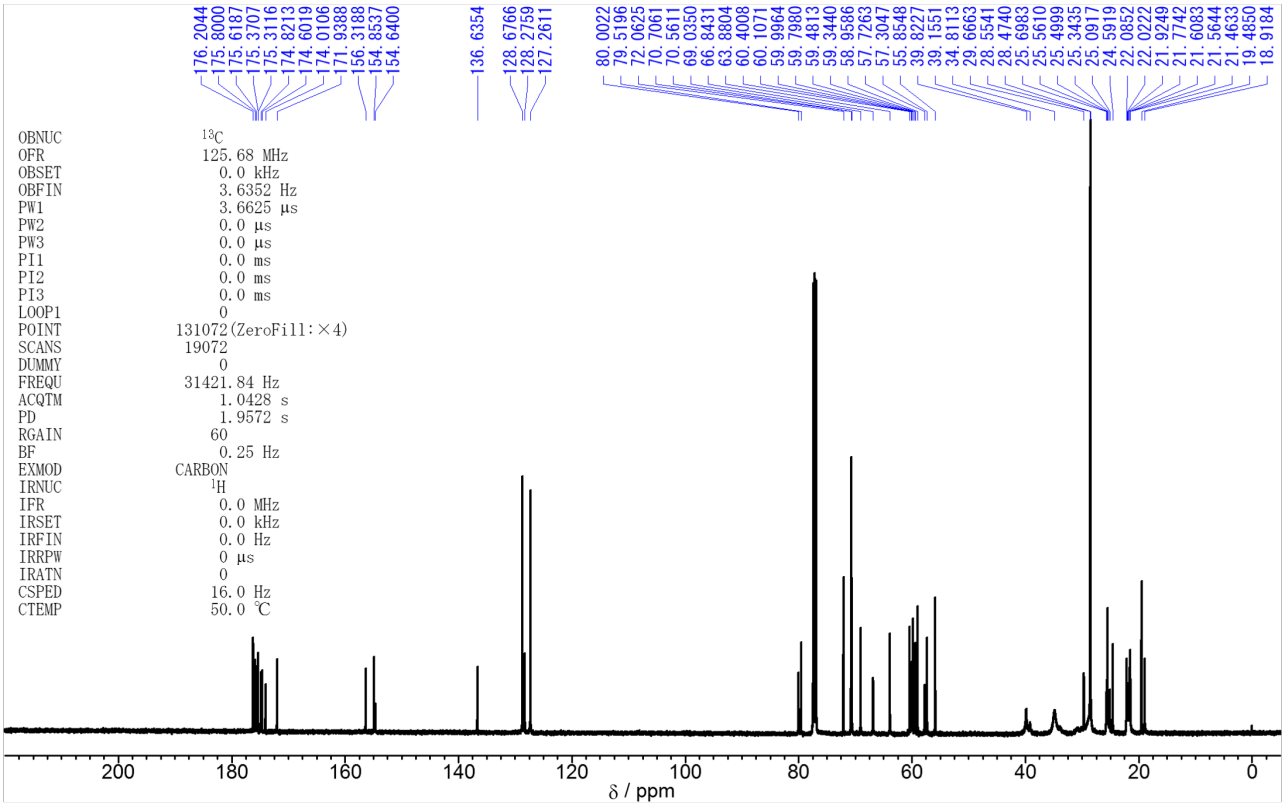

Fig. S31 ^{13}C NMR spectrum of Z-Ac$_6$c-[Api(Boc)-(Ac$_6$c)$_2$]$_2$-L-Val-Aib-OTg (**6**) in $CDCl_3$ at 50 ºC.

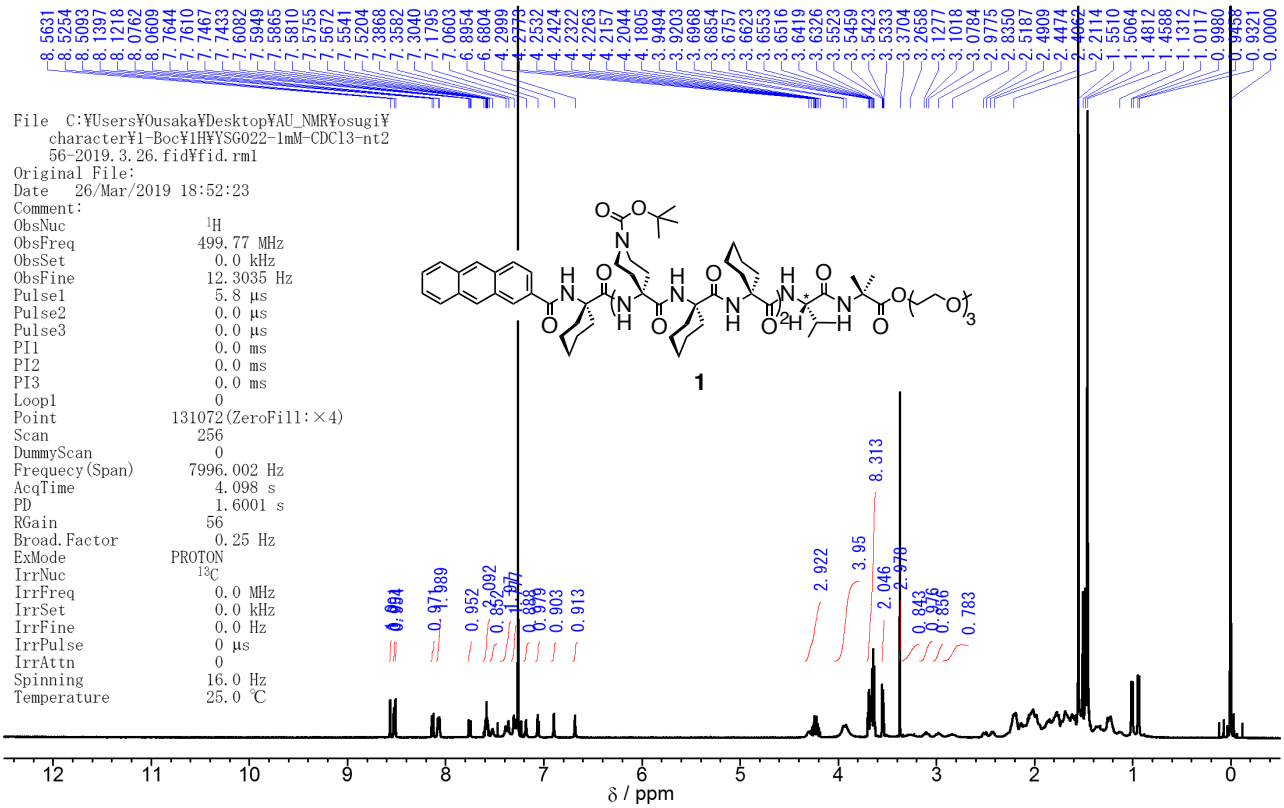

Fig. S32 ^{1}H NMR spectrum of **1** in $CDCl_3$ at 25 ºC.

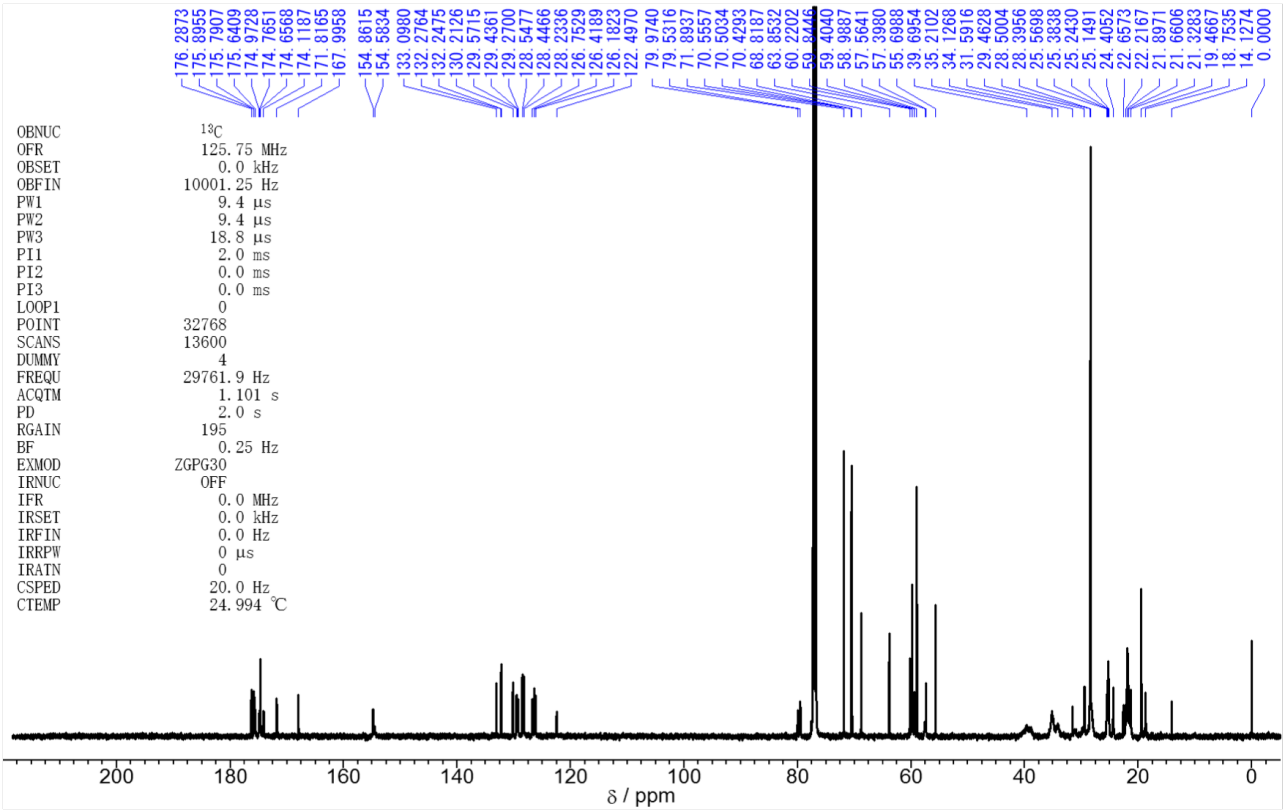

Fig. S33 ^{13}C NMR spectrum of **1** in $CDCl_3$ at 25 ºC.

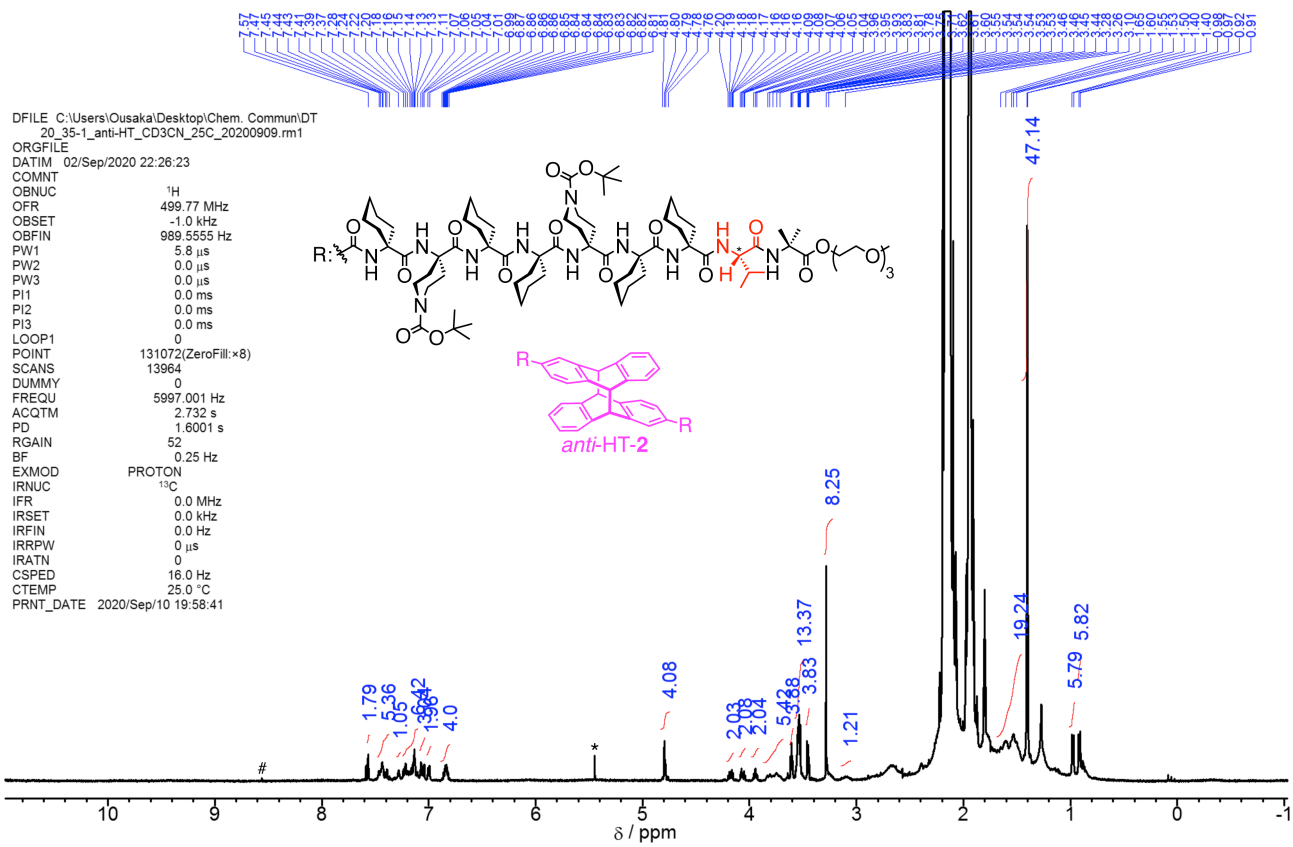

Fig. S34 ^{1}H NMR spectrum of *anti*-HT-**2** in CD_3CN at 25 ºC. The aliphatic protons are partially overlapping with H_2O and CH_3CN signals. * and # denote CH_2Cl_2 and unknown peaks, respectively.

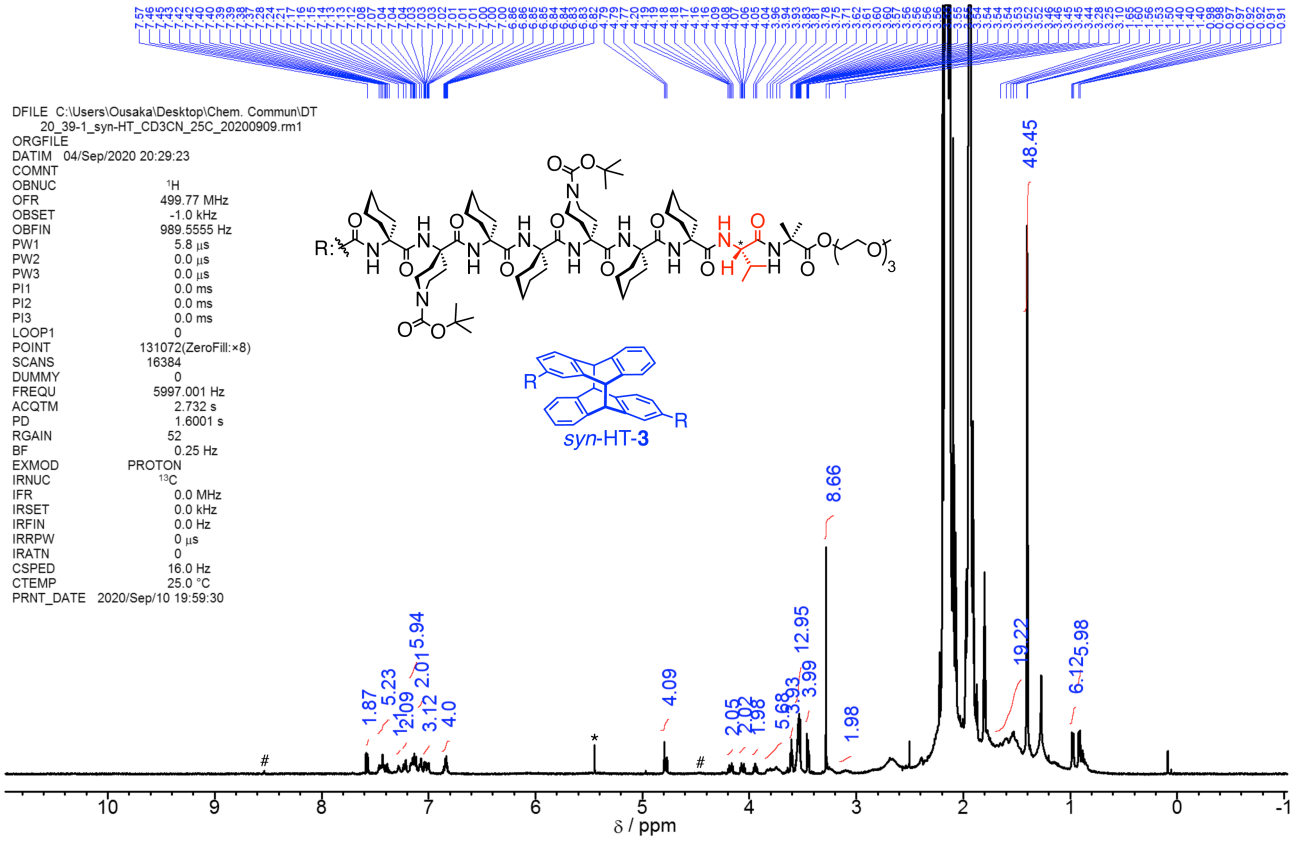

Fig. S35 ^{1}H NMR spectrum of *syn*-HT-**3** in CD_3CN at 25 ºC. The aliphatic protons are partially overlapping with H_2O and CH_3CN signals. * and # denote CH_2Cl_2 and unknown peaks, respectively.

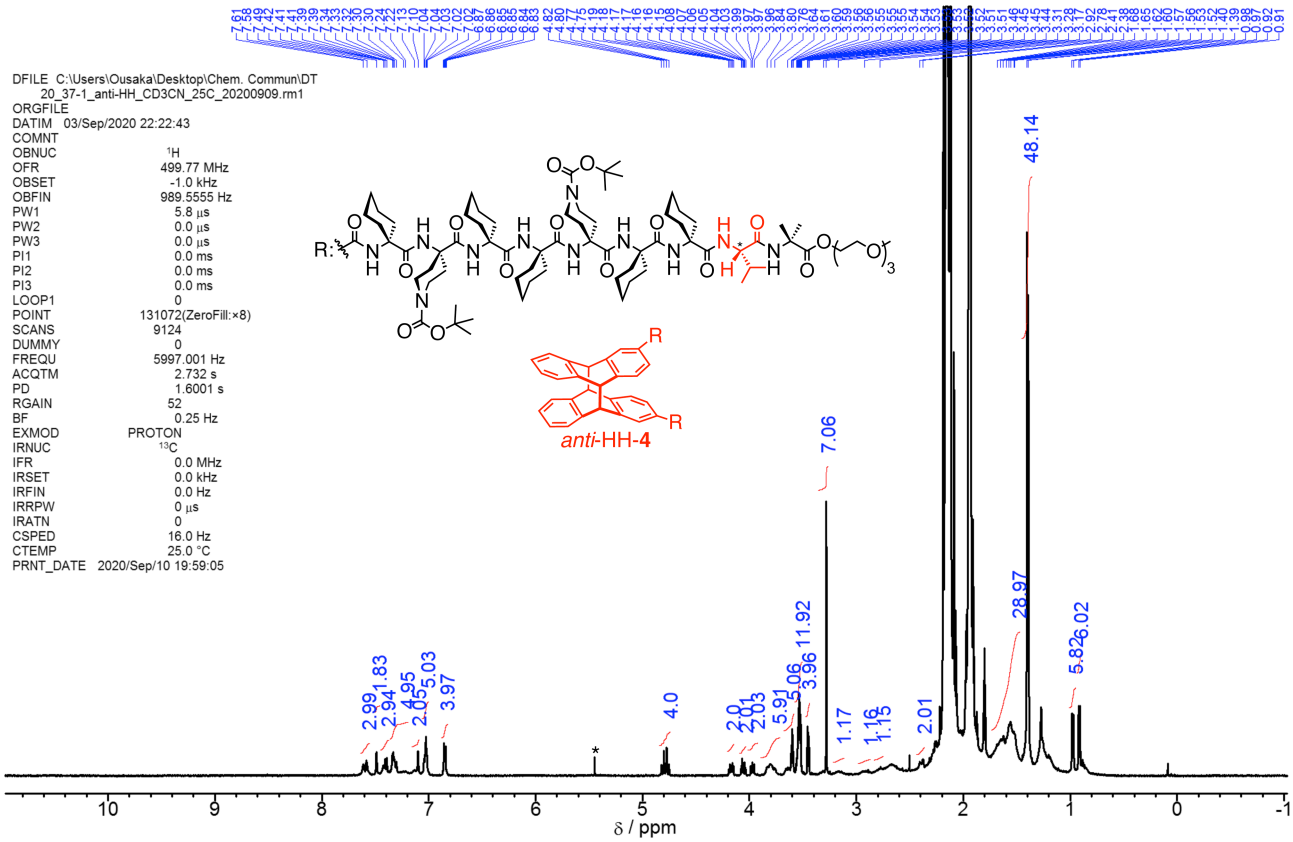

Fig. S36 ^{1}H NMR spectrum of *anti*-HH-**4** in CD_3CN at 25 ºC. The aliphatic protons are partially overlapping with H_2O and CH_3CN signals. * and # denote CH_2Cl_2 and unknown peaks, respectively.

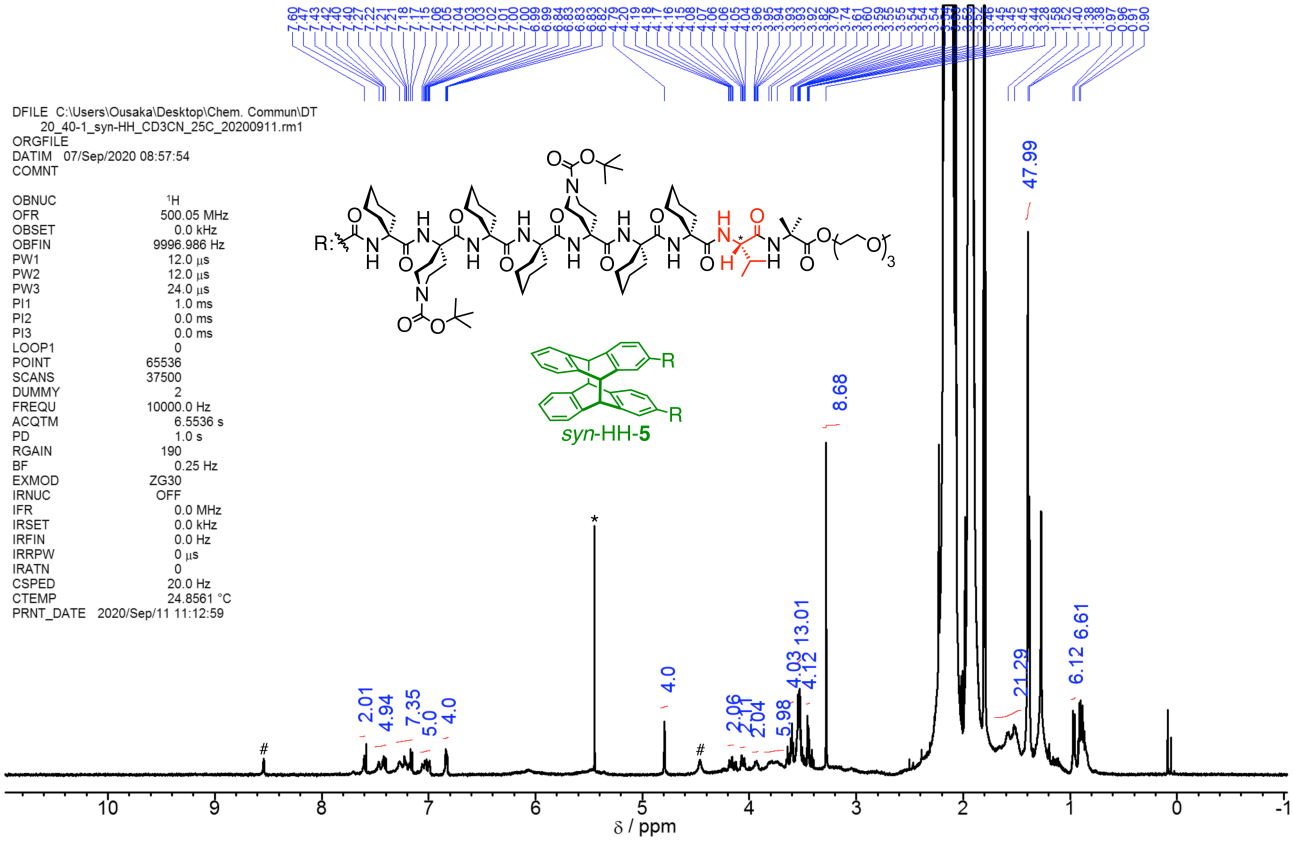

Fig. S37 ^{1}H NMR spectrum of *syn*-HH-**5** in CD_3CN at 25 ºC. The aliphatic protons are partially overlapping with H_2O and CH_3CN signals. * and # denote CH_2Cl_2 and unknown peaks, respectively.